

# Dynamics of accretion discs

Geoffroy Lesur

*with thanks to*

William Béthune (DAMTP)  
Antoine Riols (IPAG)  
Matthew Kunz (Princeton)  
François Ménard (IPAG)  
Jonathan Ferreira (IPAG)  
Sébastien Fromang (CEA)

WITGAF  
Cargese, 15 July 2019

What is the most efficient way to convert the rest mass energy of matter into heat?

A- Burning fuel  $4 \times 10^{-8} \%$

B- Nuclear fission 0.09 %

C- Nuclear fusion 0.09 %

D- ?



Accretion disc around a black hole:  
up to 40% efficiency

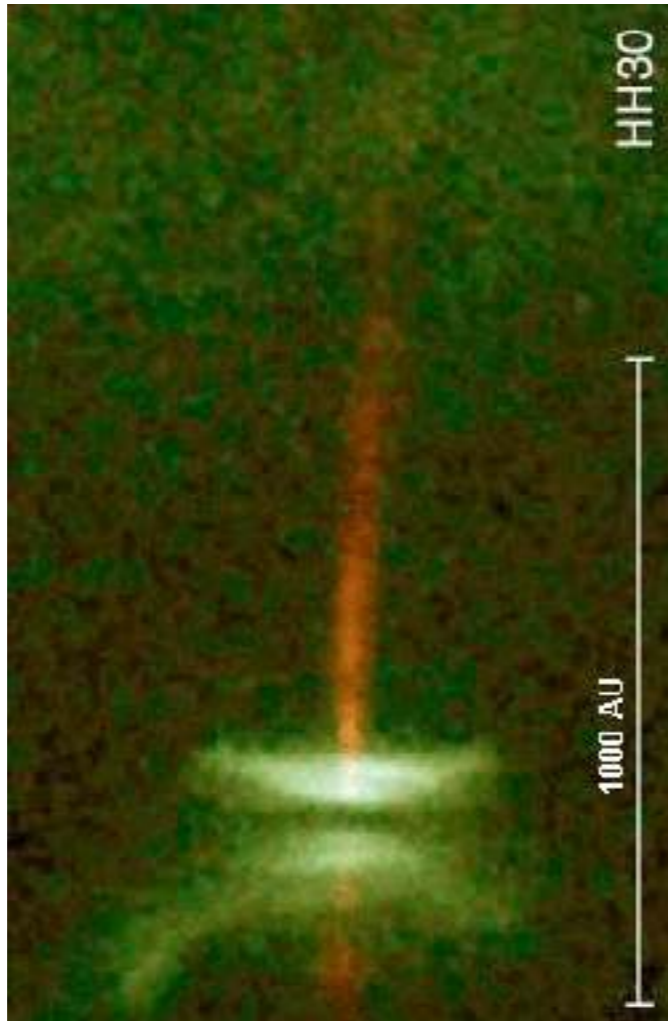
# Overview

---

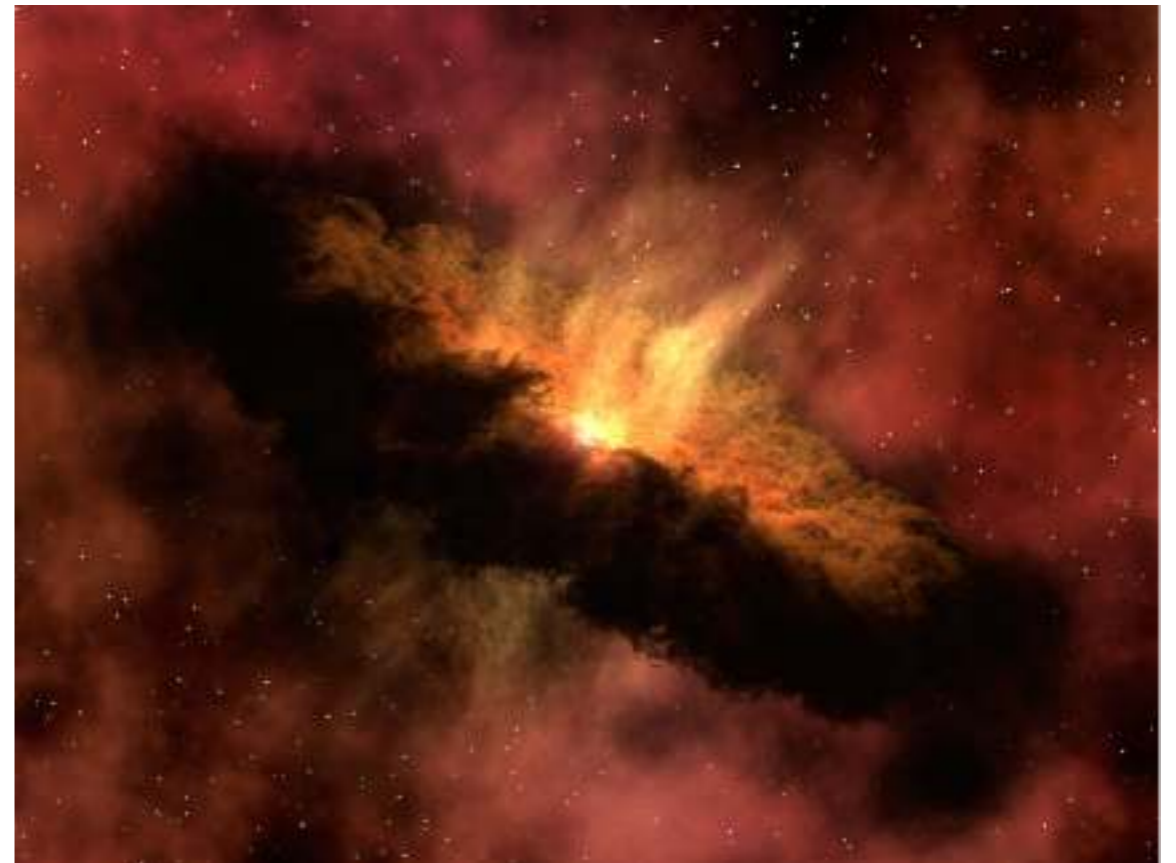
- A few fun facts about astrophysical discs (10')
- How to drive accretion (30')
- On the difficulty of driving hydrodynamic turbulence (30')
- A short introduction to magnetised wind flows (60')
- Application to protoplanetary discs (20')



# Protoplanetary discs



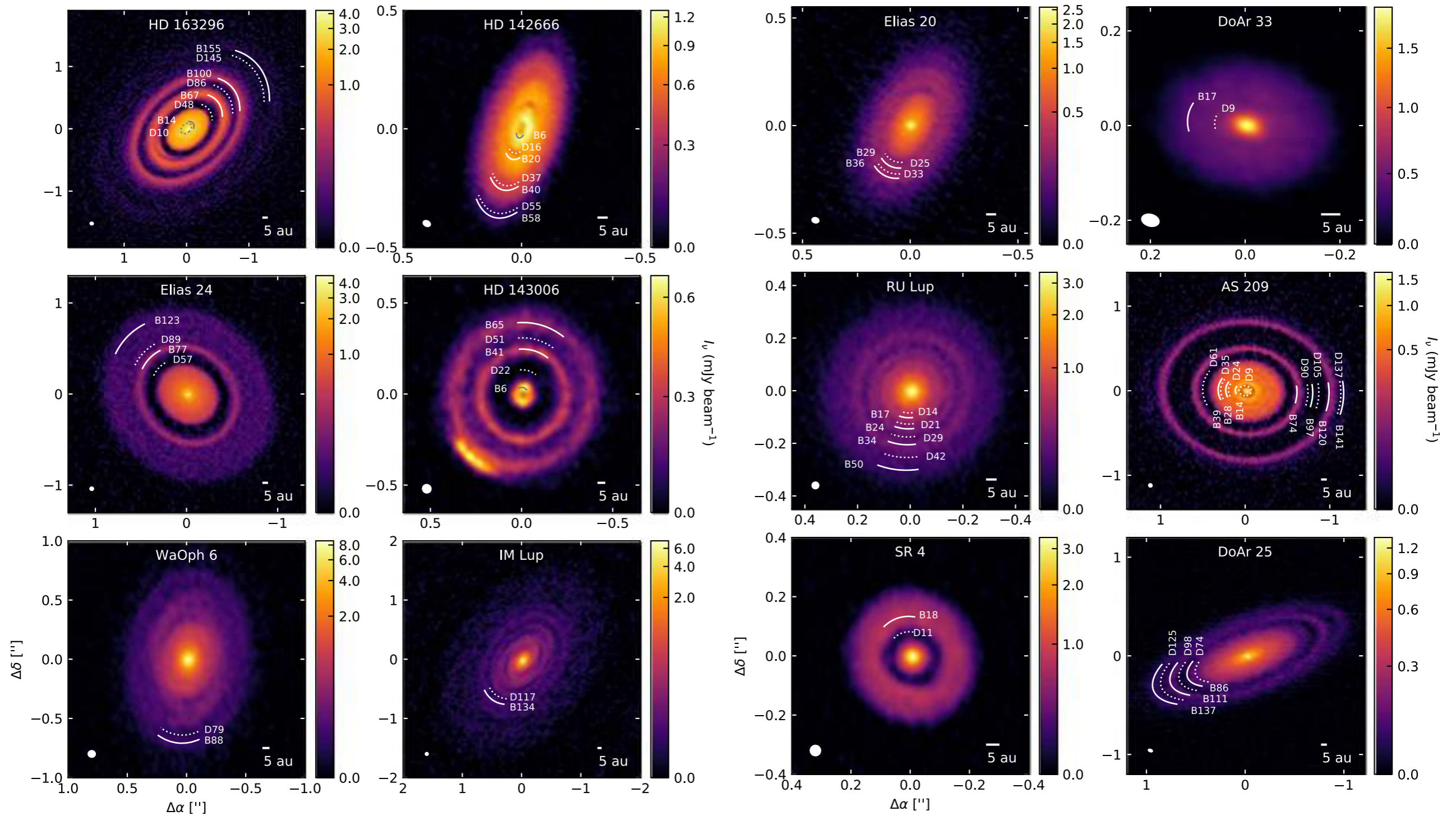
Credit: C. Burrows and J. Krist (STScI),  
K. Stapelfeldt (JPL) and NASA



Artist view

- Size  $10^9$ - $10^{13}$  m
- Central object: young star ( $10^{30}$  kg)
- Temperature  $10^3$ - $10$  K

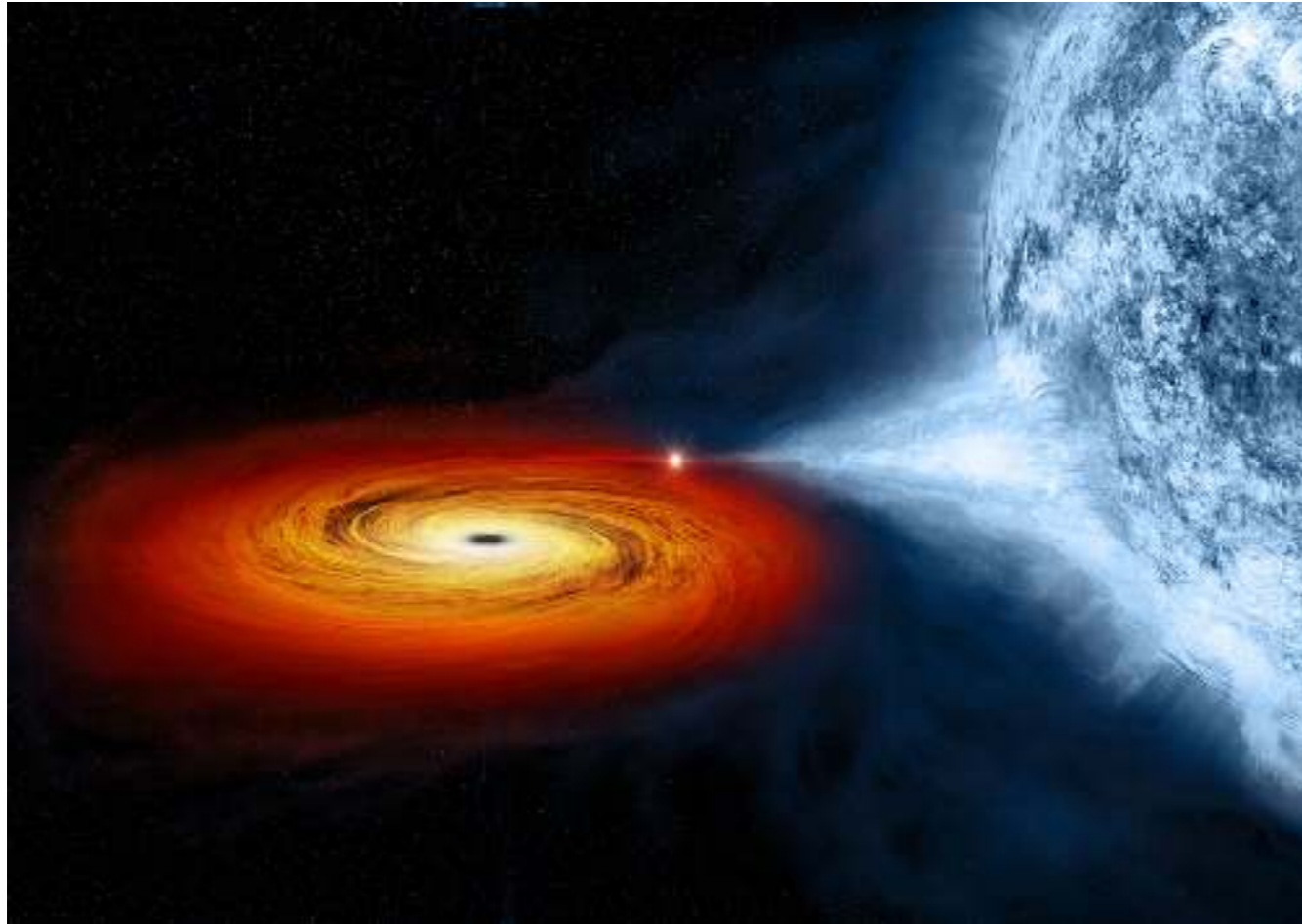
# Structures in protoplanetary discs



[Huang+ 2018]

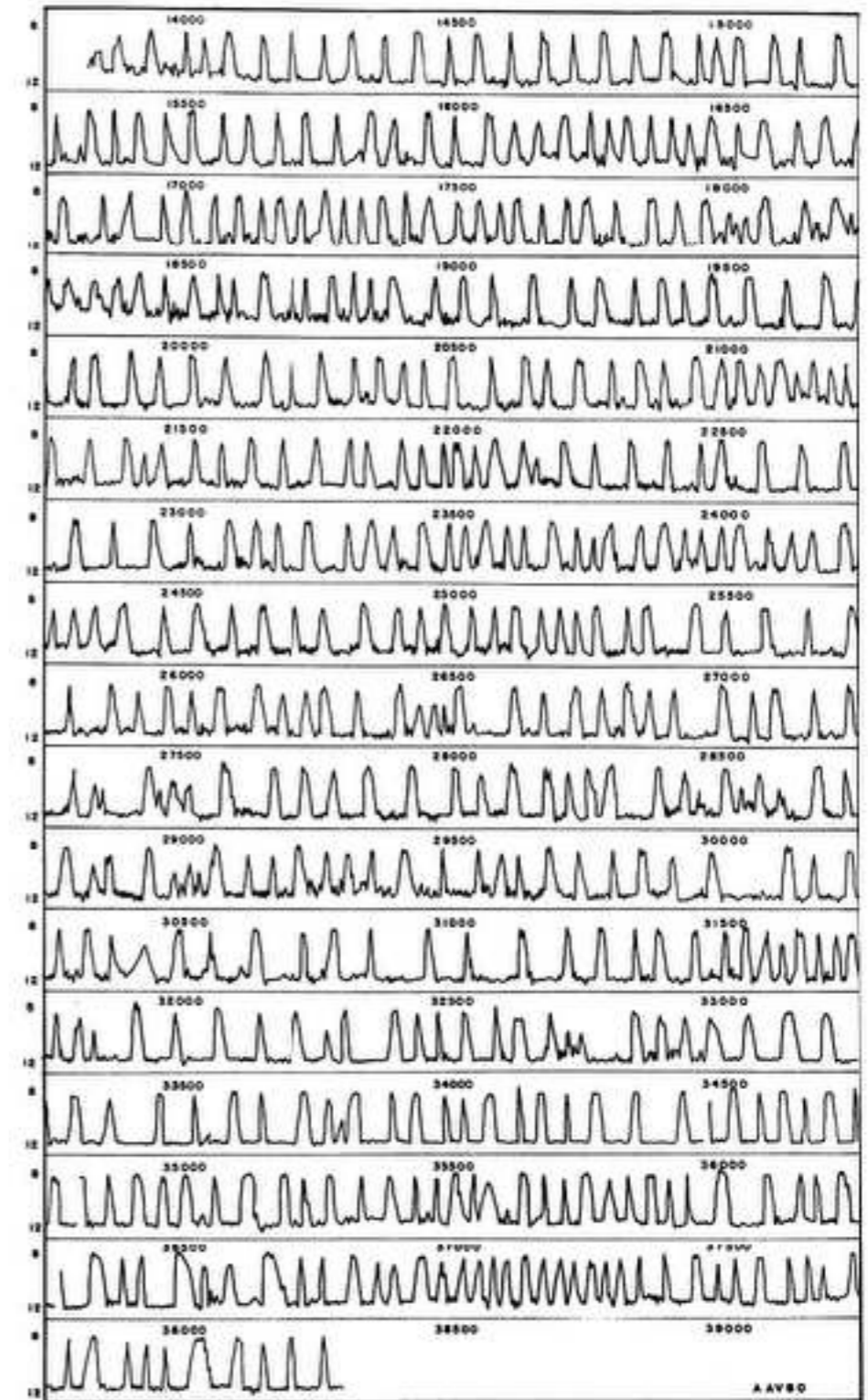


# Compact binaries



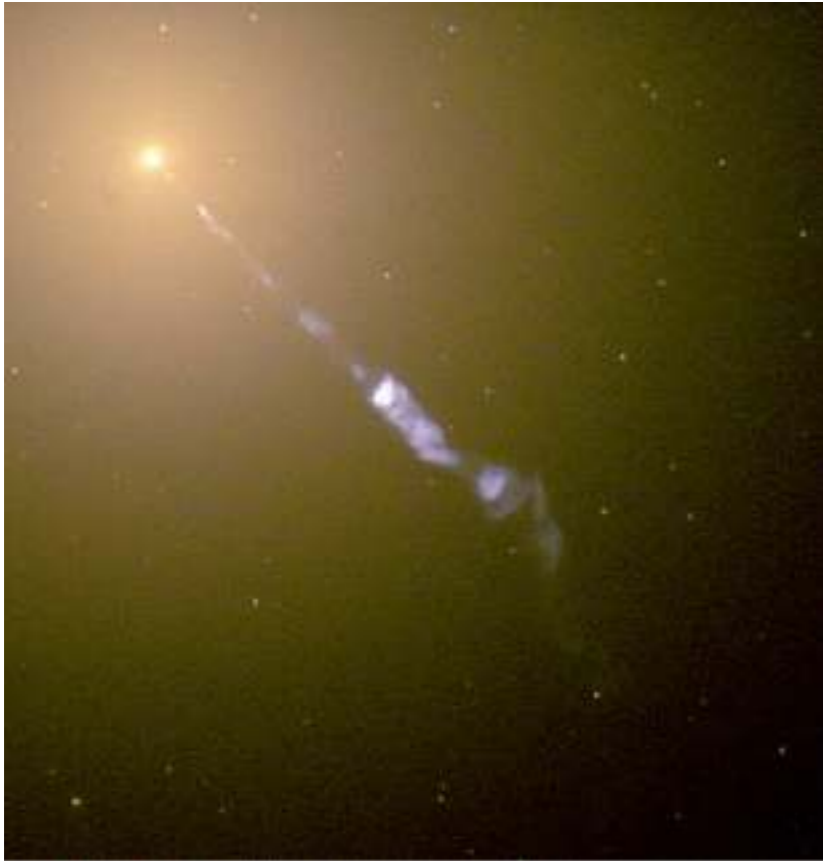
Artist view

- Size  $10^4$ - $10^8$  m
- Central object: white dwarf, neutron star, black hole ( $10^{30}$  kg)
- Temperature  $10^5$ - $10^3$  K

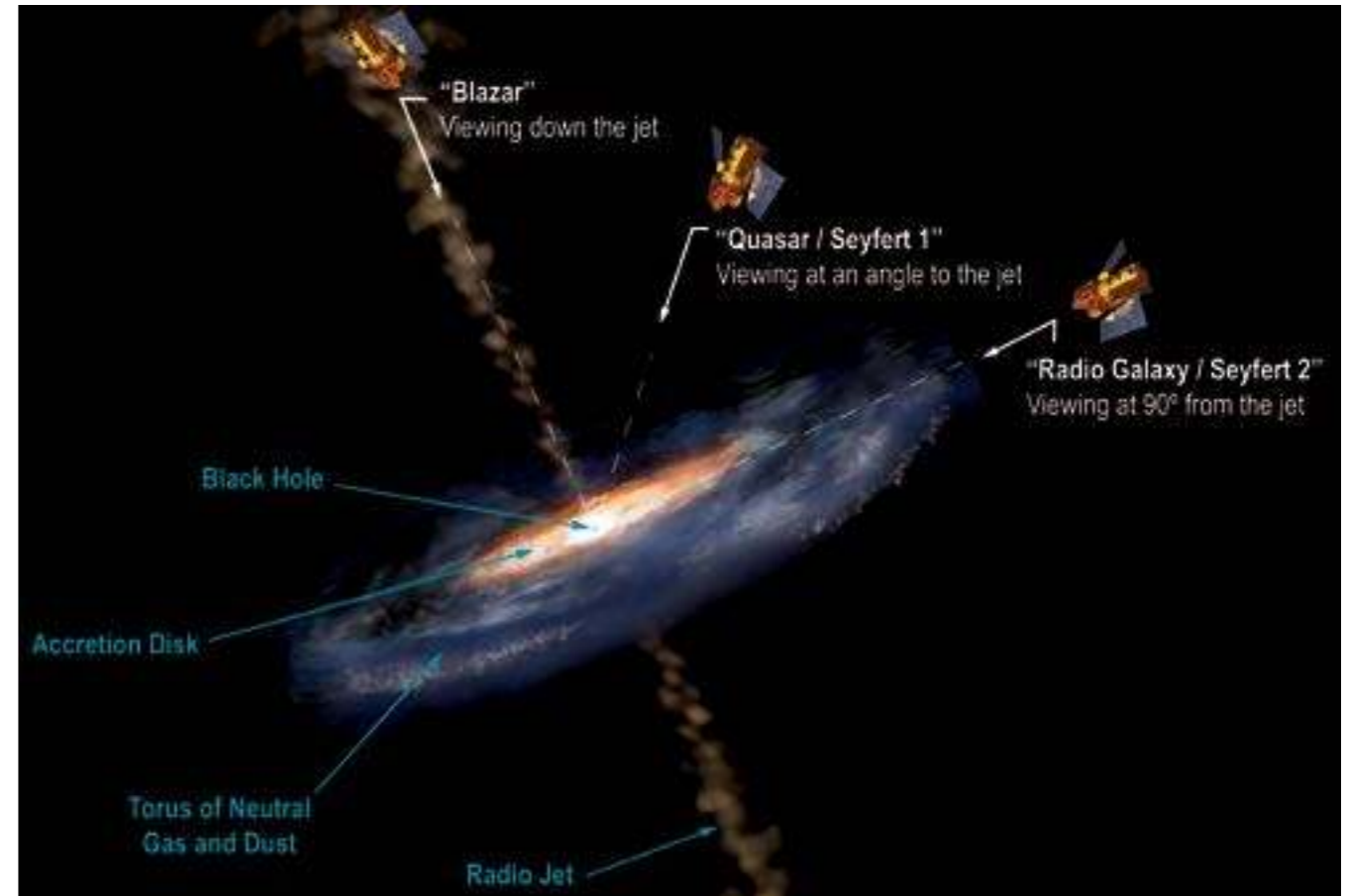


LIGHT CURVE OF SS CYGNI  
1896 — 1963

# Active galactic nuclei (blazars, quasars...)



M87



- Size  $10^{10}$ - $10^{15}$  m
- Central object: black hole ( $10^{36}$ - $10^{39}$  kg= $10^6$ - $10^9$   $M_{\text{sun}}$ )
- Temperature  $10^5$ - $10^2$  K

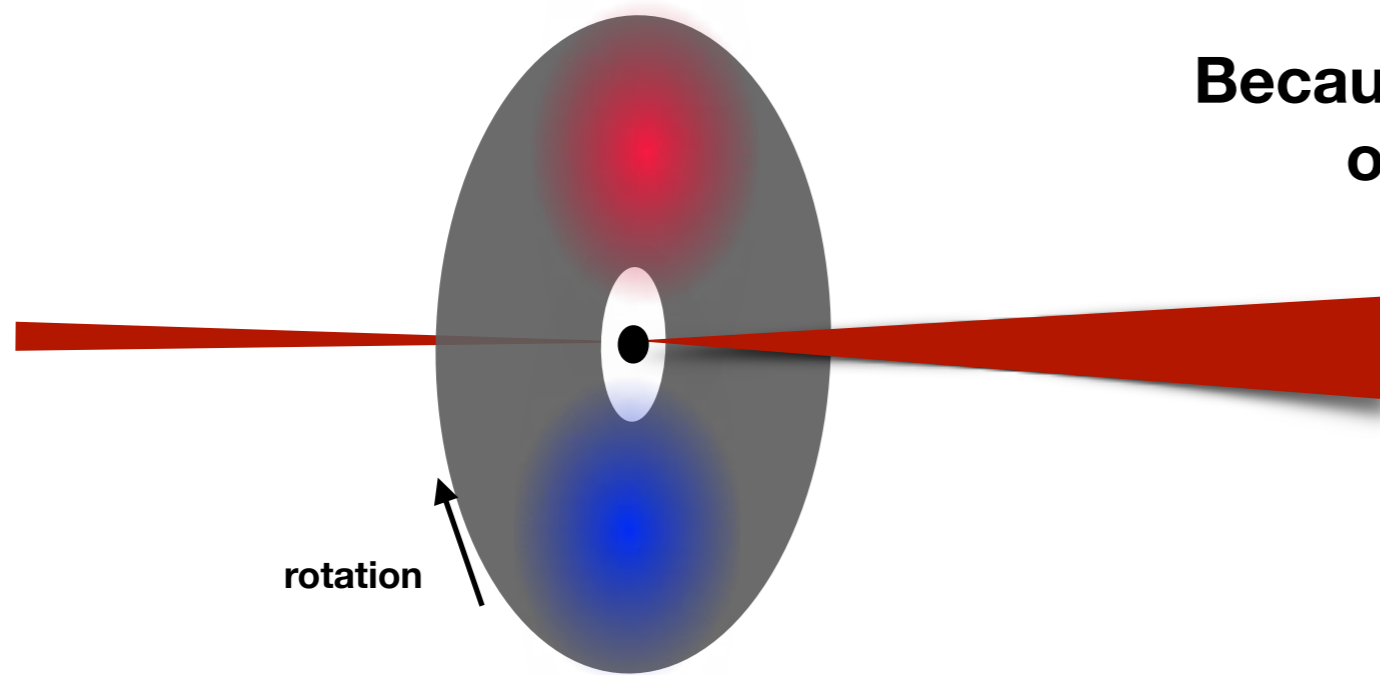


# M87: staring at a supermassive black hole

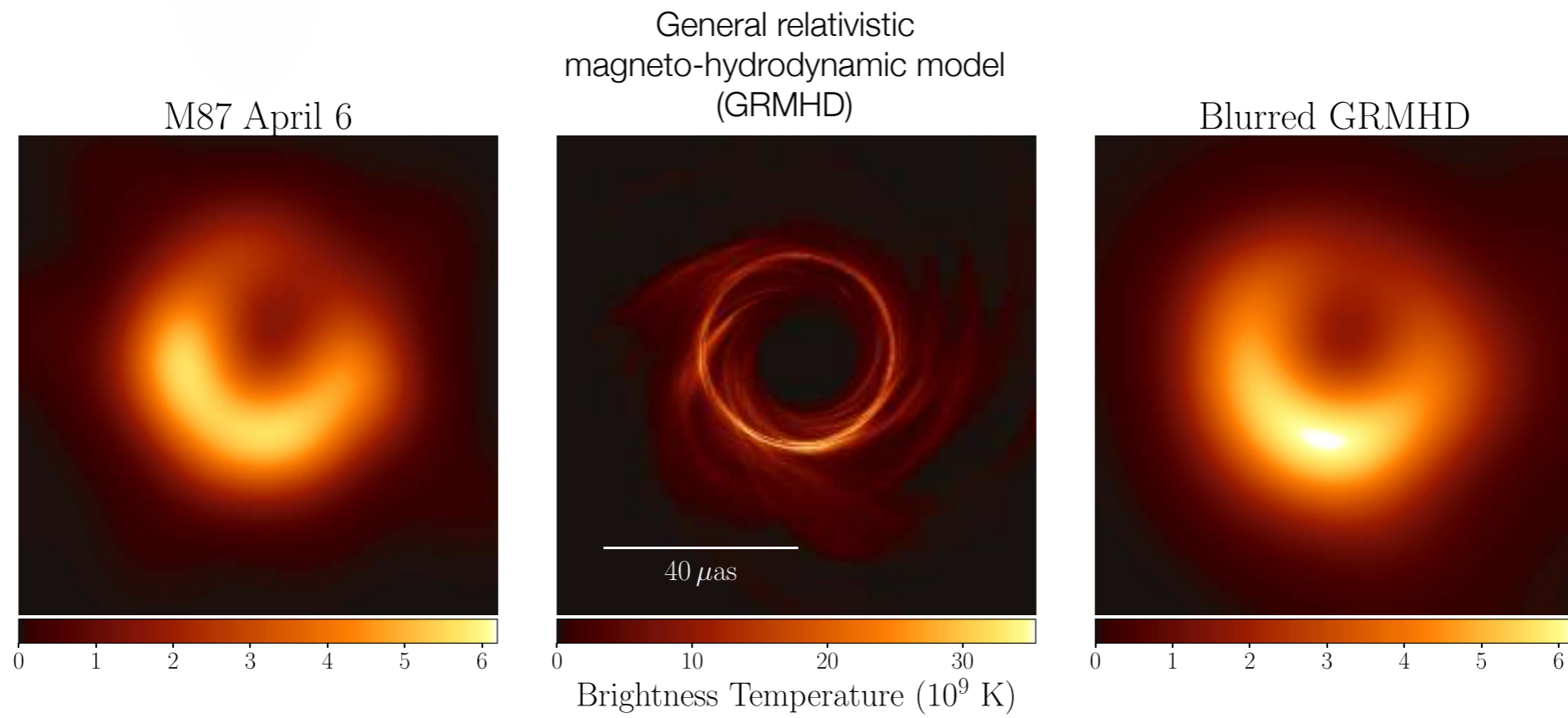




# Model of M87



**Because rotation velocities are relativistic, one expects Doppler beaming in the blue shifted region**



# Overview

---

- A few fun facts about astrophysical discs (10')
- How to drive accretion (30')
- On the difficulty of driving hydrodynamic turbulence (30')
- A short introduction to magnetised wind flows (60')
- Application to protoplanetary discs (20')



# Equations of motion

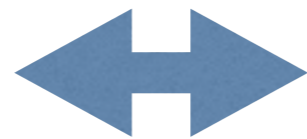
$$\frac{\partial \rho}{\partial t} + \nabla \cdot \rho \mathbf{u} = 0$$

$$\rho \left( \frac{\partial \mathbf{u}}{\partial t} + \mathbf{u} \cdot \nabla \mathbf{u} \right) = -\nabla \left( P + \frac{B^2}{8\pi} \right) + \frac{\mathbf{B} \cdot \nabla \mathbf{B}}{4\pi}$$

Magnetic pressure

Magnetic tension

$$\frac{\partial \mathbf{B}}{\partial t} = \nabla \times (\mathbf{u} \times \mathbf{B})$$



$$\frac{\partial \mathbf{B}}{\partial t} + \mathbf{u} \cdot \nabla \mathbf{B} = \mathbf{B} \cdot \nabla \mathbf{u} - \mathbf{B} \nabla \cdot \mathbf{u}$$

Transport

Warping

Compression

# Disc Dynamics

## Radial equilibrium

### Radial equilibrium

$$\frac{\partial u_r}{\partial t} + \mathbf{u} \cdot \nabla u_r - \frac{u_\phi^2}{R} = \frac{\mathbf{B} \cdot \nabla B_r}{4\pi\rho} - \frac{B_\phi^2}{4\pi\rho R} - \frac{1}{\rho} \frac{\partial (P + B^2/8\pi)}{\partial R} - \frac{GM_\odot}{R^2}$$

- Assume a thin, weakly magnetised disc

$$v_A \ll u_\phi$$

$$c_s \ll u_\phi$$

$$(u_r, u_z) \ll u_\phi$$

$$\longrightarrow u_\phi = R\Omega(R) \quad \text{with} \quad \Omega(R) = (GM_\odot)^{1/2} R^{-3/2}$$

- Disc temporal evolution dictated by small deviations from the Keplerian profile:

$$\mathbf{u} = \mathbf{v} + R\Omega(R)\mathbf{e}_\phi$$



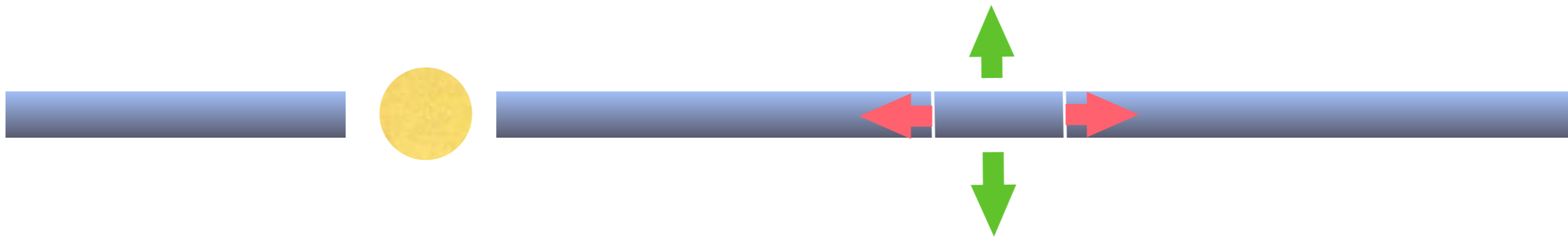
# Disc Dynamics

## Mass conservation

$$\frac{\partial \rho}{\partial t} + \nabla \cdot \rho \mathbf{u} = 0$$

Introduce:  $\bar{Q} = \int d\phi \int_{z=-h}^{z=+h} dz Q$  and  $\Sigma = \bar{\rho}$

→  $\frac{\partial \Sigma}{\partial t} + \frac{1}{R} \frac{\partial}{\partial R} R \overline{\rho v_r} + \left[ \rho v_z \right]_{z=-h}^{+h} = 0$



# Disc Dynamics

## Angular momentum conservation

Angular momentum conservation:

$$\frac{\partial(\rho R u_\phi)}{\partial t} + \nabla \cdot \left[ \rho R u_\phi \mathbf{u} - R \frac{B_\phi \mathbf{B}}{4\pi} + R \left( P + \frac{B^2}{8\pi} \right) \mathbf{e}_\phi \right] = 0$$

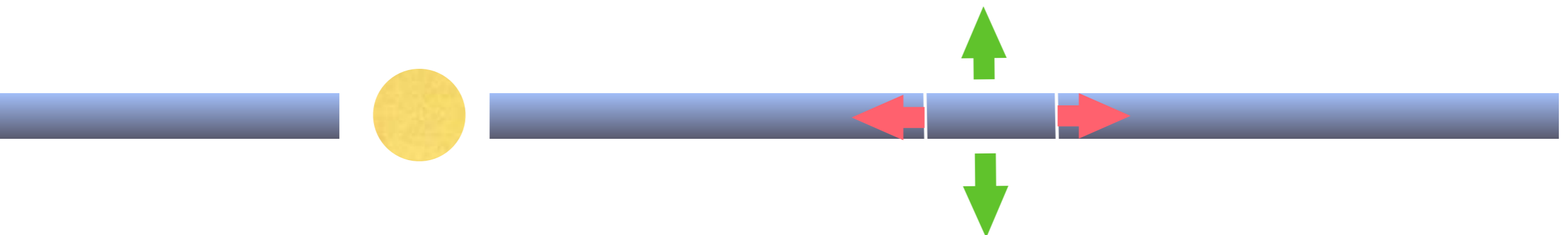
Combine it with mass conservation, squeeze it, stretch it:

$$\overline{\rho v_r} \frac{\partial}{\partial R} \Omega R^2 + \frac{1}{R} \frac{\partial}{\partial R} R^2 \left[ \overline{\rho v_\phi v_r} - \frac{\overline{B_\phi B_r}}{4\pi} \right] + R \left[ \overline{\rho v_\phi v_z} - \frac{B_\phi B_z}{4\pi} \right]_{z=-h}^{+h} = 0$$

accretion

radial stress

vertical stress  
(aka wind stress)





# Disc Dynamics

alpha disc model

[Shakura-Sunyaev 1973]

- Introduce the dimensionless number

$$\alpha = \frac{\overline{\rho v_{\phi} v_r} - \overline{B_{\phi} B_r} / 4\pi}{\Sigma \Omega^2 H}$$

- Estimated accretion rate

$$\overline{\rho v_r} \sim -\alpha c_s \Sigma \frac{H}{R}$$

- Compare to observations:  $10^{-4} < \alpha < 10^{-1}$

*New questions!*

- What is responsible for anomalous viscosity?
- How large is  $\alpha$  ?
- What about winds ?

# The zoo of disc instabilities

[see Fromang & Lesur 2017  
for a complete review]

## Local instabilities:

- Magnetorotational instability (MRI): shear driven instability but requires an ionised plasma  
(Velikhov 1959, Chandrasekhar 1960, Balbus & Hawley 1991) **COVERED BY C. BARUTEAU**
- Gravitational instabilities: only for massive & cold enough disc  
(Gammie 2001, Paardekooper 2012) **COVERED BY C. BARUTEAU**
- Subcritical shear instability: probably not efficient enough, if it exists (see later)  
(Lesur & Longaretti 2005, Scharfman et al. 2012, Edlund & Ji 2014)
- Vertical Shear instability: driven by vertical shear (actually link to the baroclinicity of the disc)  
(Urpin & Brandenburg (1998), Nelson+ 2013, Barker & Latter 2015) **COVERED BY C. BARUTEAU**
- « Baroclinic » instabilities (SBI, convective overstability): requires a radially unstable entropy profile  
(Petersen+ 2007, Lesur & Papaloizou 2010, Klahr & Hubbard 2014) **COVERED BY C. BARUTEAU**
- Zombie vortex instability: buoyancy critical layer instability  
(Marcus+ 2013, Marcus+2016, Lesur & Latter 2016)
- Rossby wave instability: requires a local maximum of vortensity (equivalent to Kelvin-Helmholtz)  
(Lovelace et. al 1999) **COVERED BY C. BARUTEAU**
- Vertical convective instability: Requires a heat source in the midplane  
(Cabot 1996, Lesur & Ogilvie 2010, Held & Latter 2018)

## Global instabilities:

- Papaloizou & Pringle instability: density wave reflection on the inner edge  
(Papaloizou & Pringle 1985)

# Overview

---

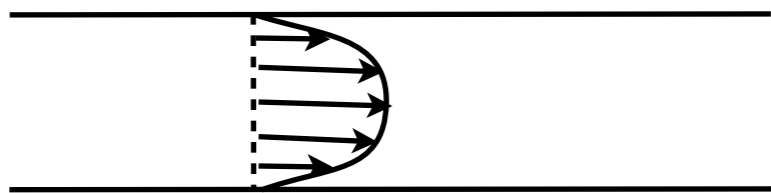
- A few fun facts about astrophysical discs (10')
- How to drive accretion (30')
- On the difficulty of driving hydrodynamic turbulence (30')
- A short introduction to magnetised wind flows (60')
- Application to protoplanetary discs (20')

# Subcritical shear instabilities

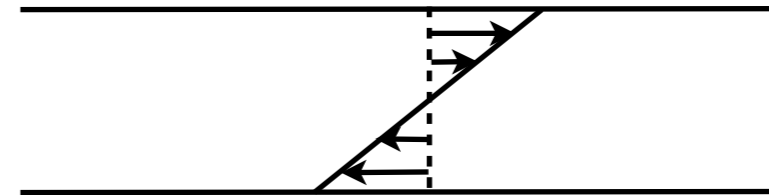
## Origins

The Facts:

- Keplerian shear flows are linearly stable
- Huge Reynolds numbers ( $10^{15}$ ) → nonlinear instability? (same thing as pipe flows or Couette flows)



pipe flow

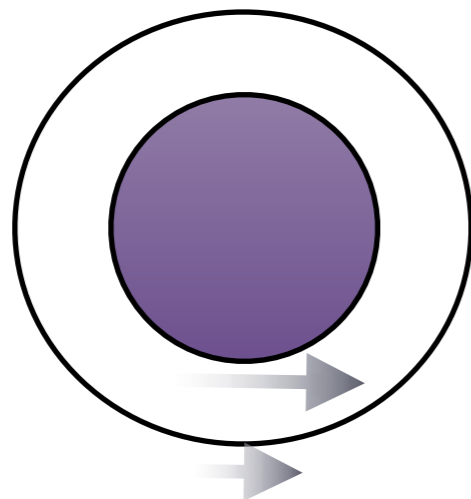


couette flow

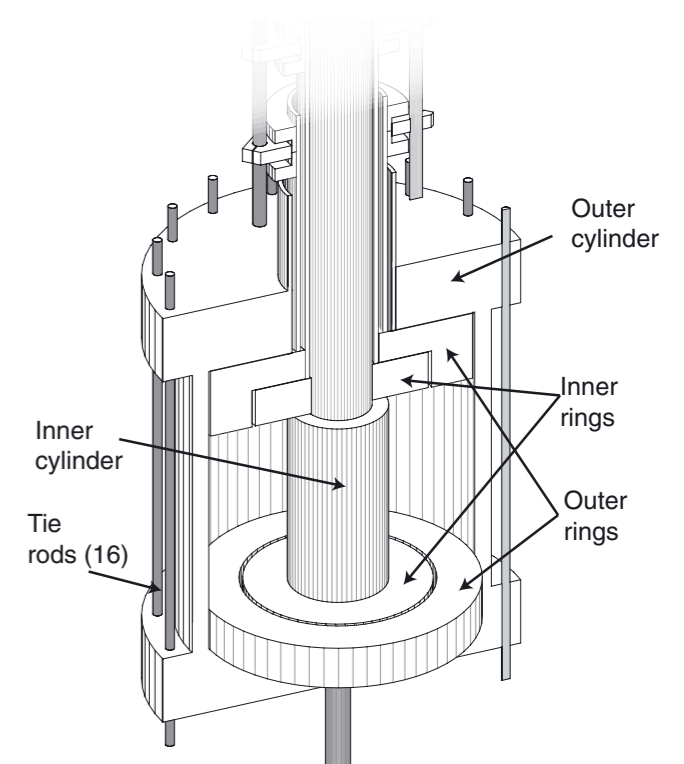
A nonlinear instability in accretion discs?

- Experimental approach: hard to «do» a disc in a lab. Boundary conditions?
- Numerical approach: high Reynolds numbers unreachable:  $Re \lesssim 10^4$

Ideal Taylor-Couette



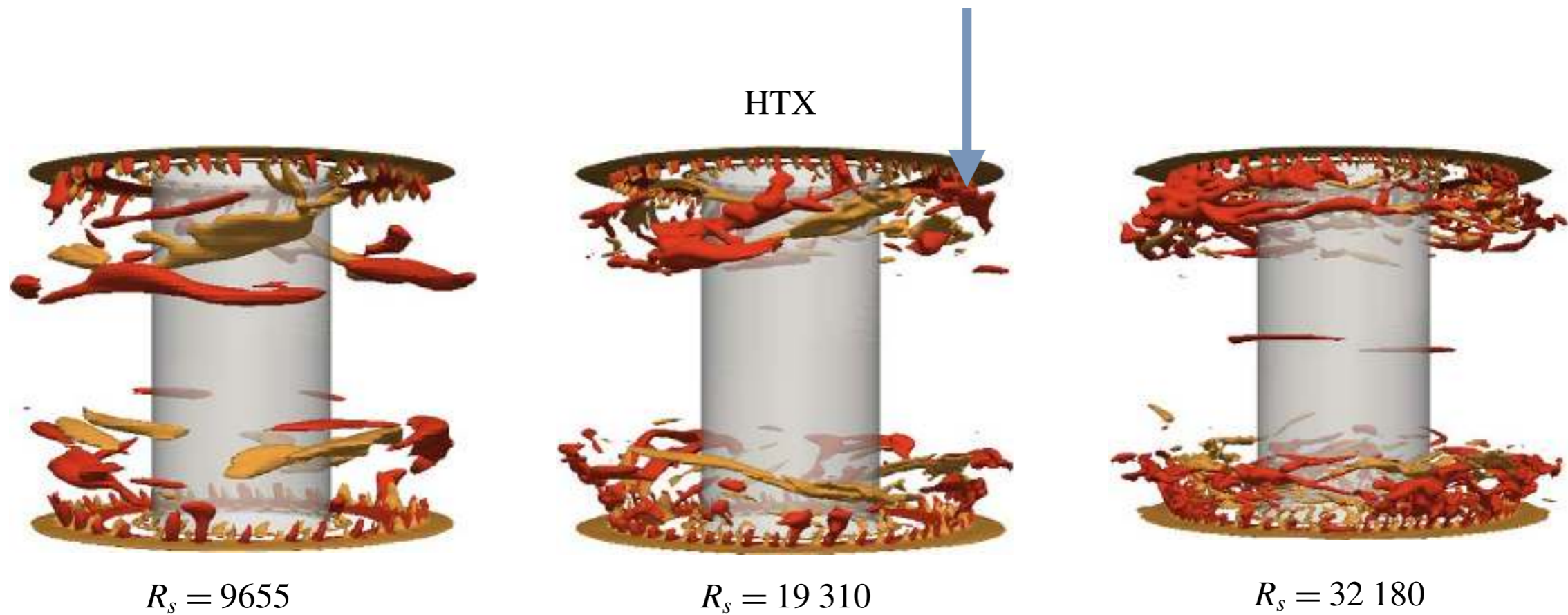
Real life  
Couette-Taylor  
(Schartman et al. 2012)





# A boundary problem

Turbulence excited by Ekman layers



Lopez & Avila (2017)

# Can non-linear, shear-driven, instabilities, if they exist, transport angular momentum efficiently in Keplerian flows?

[H. Ji]

## A contentious debate...

### Theory and simulations:

- Zeldovich (1981): maybe **yes**
- Durbulle (1993): maybe **yes**
- Balbus, Hawley & Stone (1996): **no**
- Richard & Zahn (1999): maybe **yes**
- Longaretti (2002), Chagelishvili+ (2003), Tevzadze+ (2003), Yecko (2004), Umurhan & Regev (2004), Mukhopadhyay+ (2005), Afshordi+ (2005), Dubrulle+ (2005), Ogilvie & Garaud (2005): maybe **yes**
- Lesur & Longaretti (2005): **no**
- Rincon+ 2007, Lithwick (2007, 2009), Mukhopadhyay+ (2011), Avila (2012), Mukhopadhyay & Chattopadhyay (2013): maybe **yes**
- Osticlla-Monico+ (2014): maybe **no**
- Bhatia & Mukhopadhyay (2016): maybe **yes**
- Lopez & Avila (2017), Shi+ 2017: **no**

### Laboratory experiments

- Richard & Zahn (2001): **yes**
- Beckley & Colgate (2002): maybe **no**
- Kageyama+ (2004): maybe **no**
- Ji+(2006), Scharfman+ (2012): **no**
- Paoletti & Lathrop (2011), Paoletti (2012): **yes**
- Edlund & Ji (2014): **no**
- Nordslek + (2015): maybe **no**
- Edlund & Ji (2015): **no**

Finally converging to a « no » (but no formal proof)

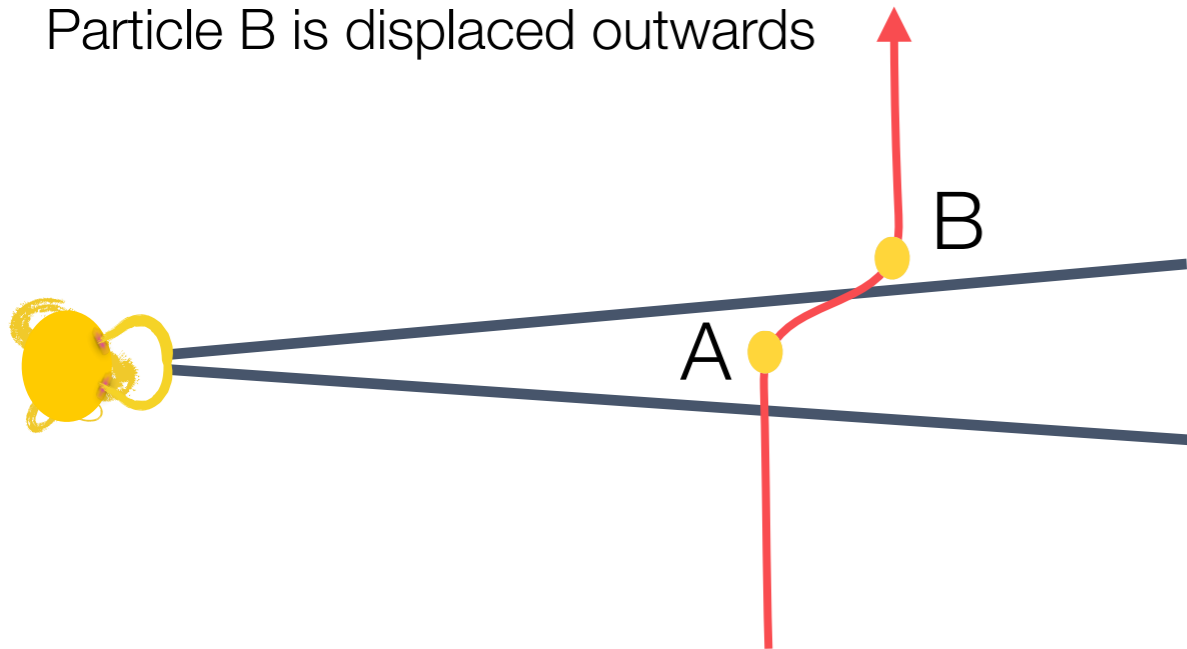
# Overview

---

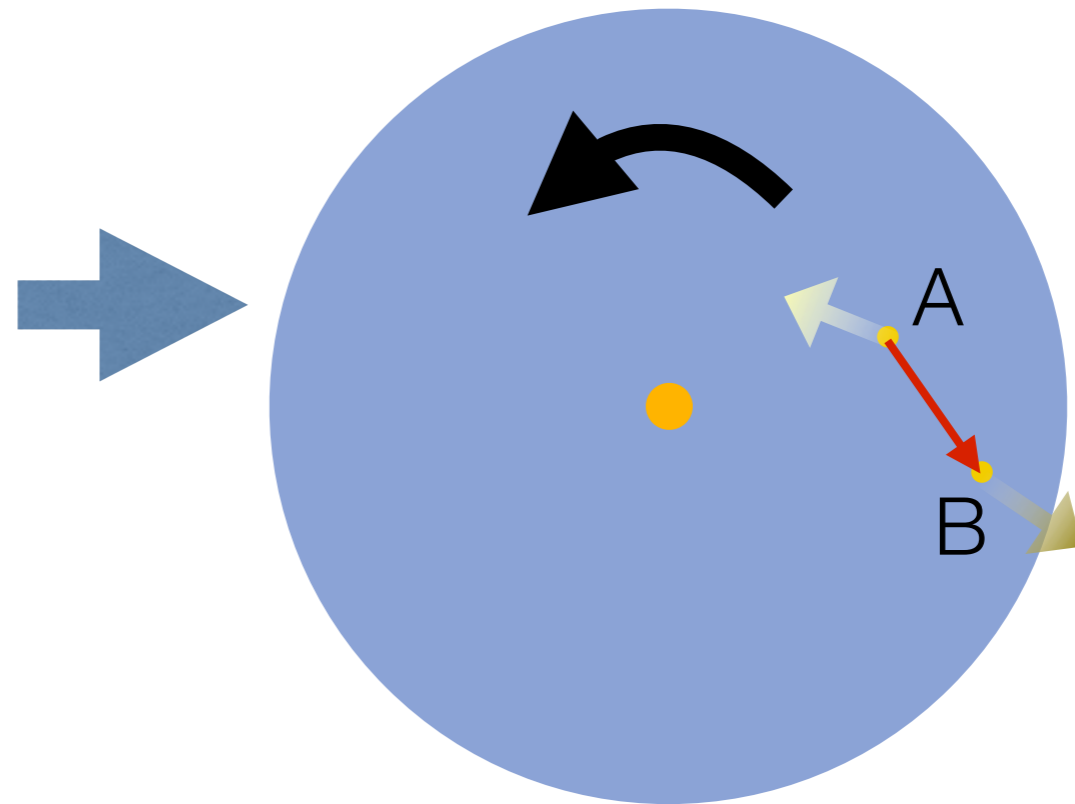
- A few fun facts about astrophysical discs (10')
- How to drive accretion (30')
- On the difficulty of driving hydrodynamic turbulence (30')
- A short introduction to magnetised wind flows (60')
- Application to protoplanetary discs (20')

# Magnetised winds: a MRI mode becoming non-linear

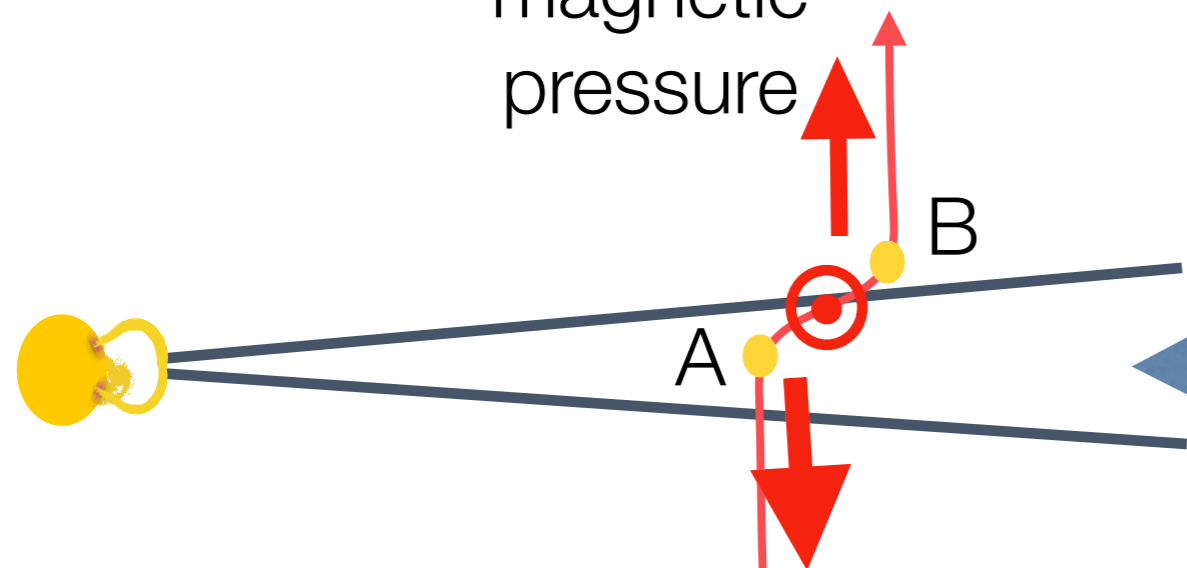
Particle A is displaced inwards,  
Particle B is displaced outwards



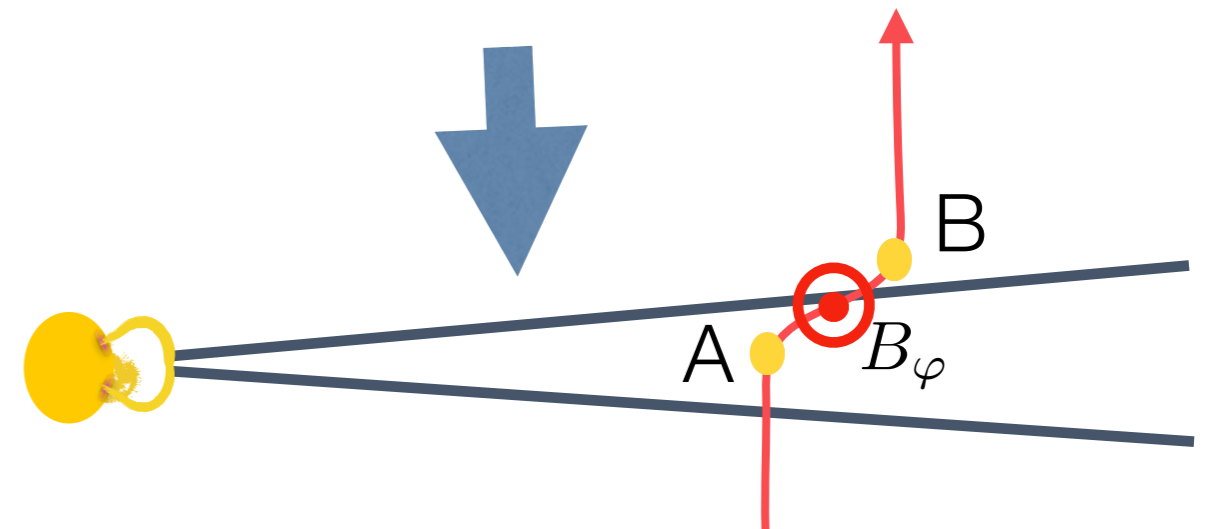
From angular momentum conservation, particle A gets  
a faster angular velocity while particle B gets slower



magnetic  
pressure



The accumulated toroidal field create a vertical magnetic  
pressure gradient, pushing B upwards and A downwards

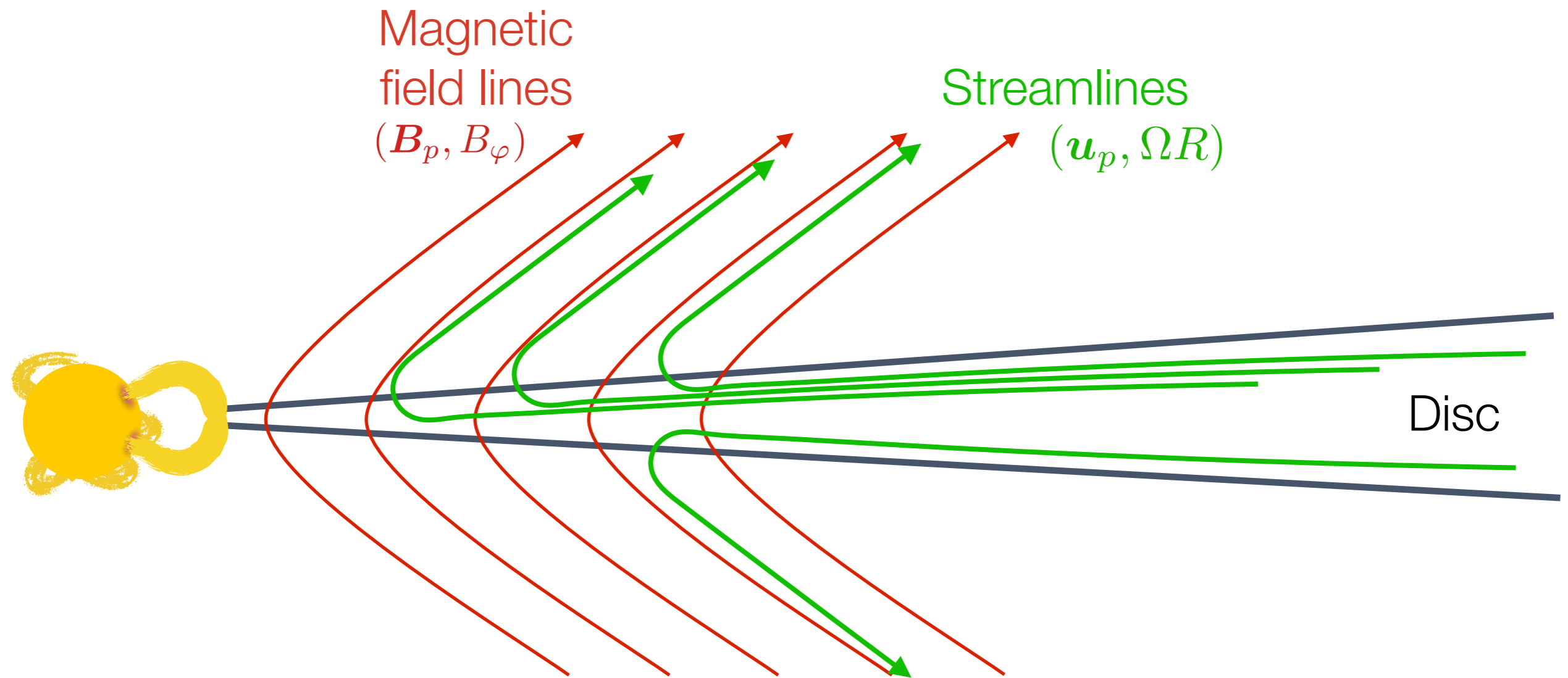


As particles A and B drift, an azimuthal  
magnetic field builds up between the particles



# Outflows

## Framework



We assume stationary, axisymmetric, ideal MHD

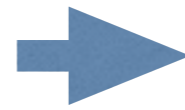
Field strength controlled by the plasma  $\beta_p = \frac{8\pi P_{\text{midplane}}}{B_z^2}$  parameter .

# Stationary equations

The need for a magnetically diffusive disc

$$\nabla \cdot \mathbf{B}_p = 0$$

(solenoidal condition)



$$\mathbf{B}_p = \frac{1}{R} \nabla a \times \mathbf{e}_\phi.$$

$$\nabla \cdot \rho \mathbf{u}_p = 0$$

(mass & solenoidal condition)

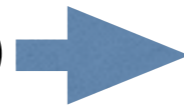
$$\rho \mathbf{u}_p \cdot \nabla u_R = \rho \Omega^2 r - \partial_R P + \frac{J_\phi B_z}{c} - \frac{J_z B_\phi}{c} - \rho \partial_R \psi \quad (\text{R-momentum})$$

$$\nabla \cdot \left( \rho \mathbf{u}_p \Omega R^2 - R \frac{\mathbf{B}_p B_\phi}{4\pi} \right) = 0 \quad (\phi\text{-momentum})$$

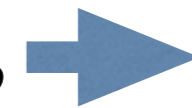
$$\rho \mathbf{u}_p \cdot \nabla u_z = -\partial_z P - \partial_z \left( \frac{B_\phi^2 + B_R^2}{8\pi} \right) + \frac{B_R \partial_R B_z}{4\pi} - \rho \partial_z \psi \quad (\text{z-momentum})$$

$$\nabla \times (\mathbf{u}_p \times \mathbf{B}_p) = 0,$$

(poloidal induction)



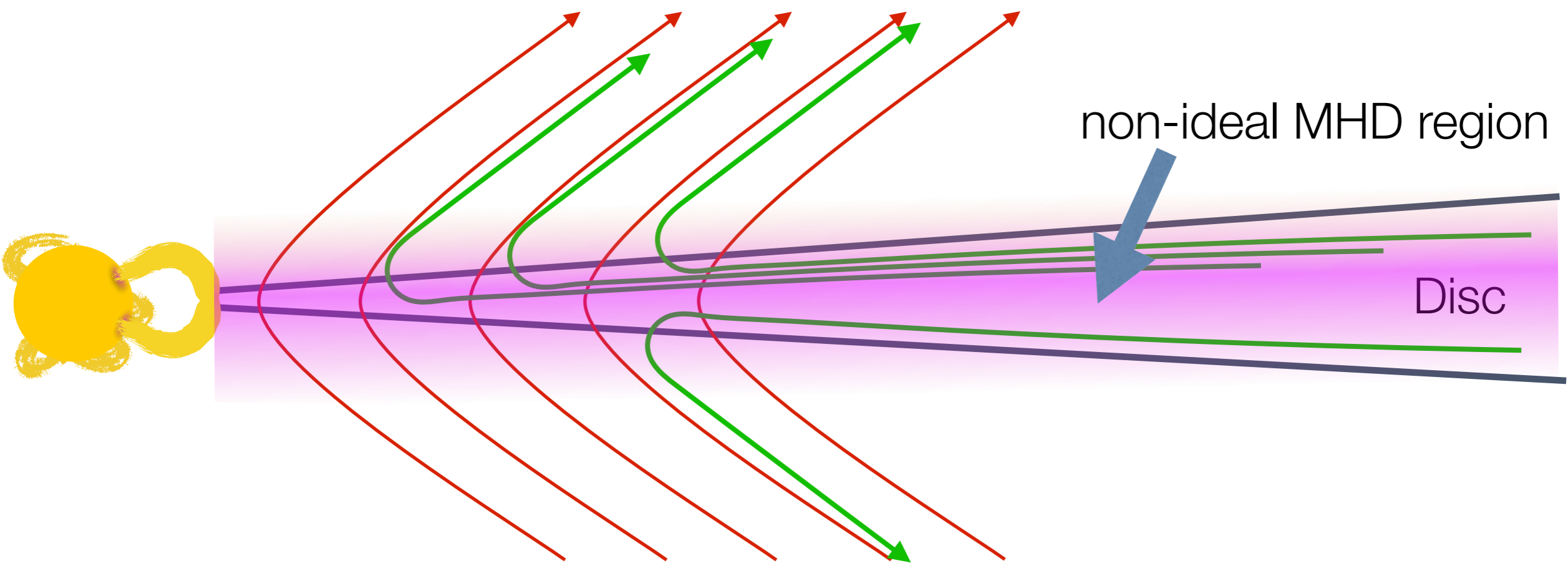
$$\mathbf{u}_p \parallel \mathbf{B}_p$$



not possible  
in the disc

$$\nabla \cdot \frac{1}{R} (\Omega R \mathbf{B}_p - B_\phi \mathbf{u}_p) = 0.$$

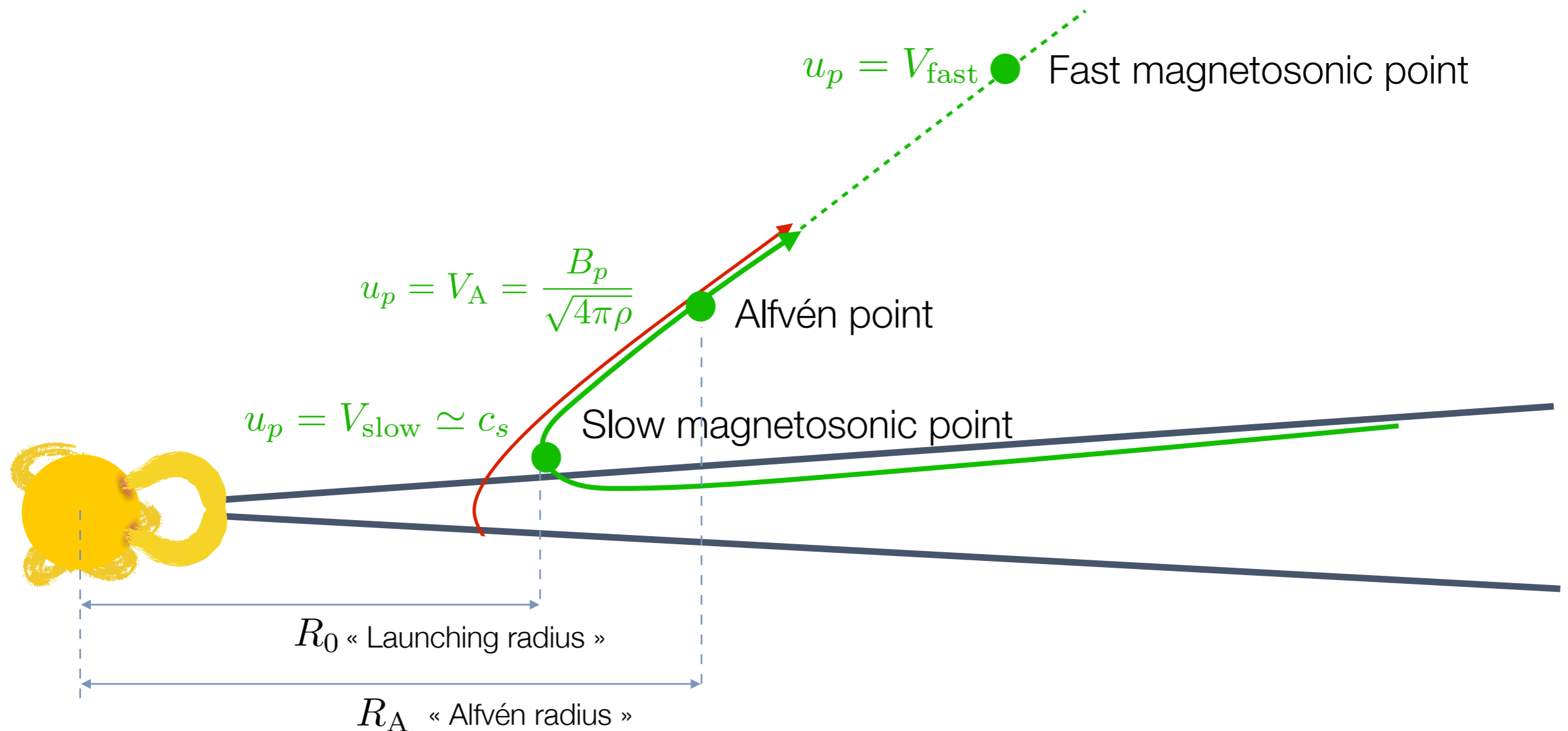
( $\phi$  induction)



# Stationary equations

## Critical points

The system of equations has 3 critical points (= critical layers for hydro people)



An outflow is causally « disconnected » from its launching point once it has crossed all three critical points

# Stationary equations

Invariants along the streamlines

[Blandford & Payne 1982]

$$\left. \begin{array}{l} \nabla \cdot \mathbf{B}_p = 0 \\ \nabla \cdot \rho \mathbf{u}_p = 0 \end{array} \right) \longrightarrow \kappa(a) \equiv \frac{\rho u_p}{B_p} \quad \text{« mass loading parameter »}$$

$$\rho \mathbf{u}_p \cdot \nabla u_R = \rho \Omega^2 r - \partial_R P + \frac{J_\phi B_z}{c} - \frac{J_z B_\phi}{c} - \rho \partial_R \psi$$

$$\nabla \cdot \left( \rho \mathbf{u}_p \Omega R^2 - R \frac{B_p B_\phi}{4\pi} \right) = 0 \longrightarrow \Omega^*(a) R_A^2 = \ell(a) \equiv \Omega R^2 - \frac{R B_\phi}{4\pi \kappa(a)} \quad \text{« angular momentum parameter »}$$

$$\rho \mathbf{u}_p \cdot \nabla u_z = -\partial_z P - \partial_z \left( \frac{B_\phi^2 + B_R^2}{8\pi} \right) + \frac{B_R \partial_R B_z}{4\pi} - \rho \partial_z \psi$$

$$\nabla \times (\mathbf{u}_p \times \mathbf{B}_p) = 0,$$

$$\nabla \cdot \frac{1}{R} (\Omega R \mathbf{B}_p - B_\phi \mathbf{u}_p) = 0 \longrightarrow \Omega^*(a) \equiv \Omega - \frac{\kappa(a)}{\rho R} B_\phi \quad \text{« rotation speed of magnetic surfaces »}$$

In addition, one can create an energy invariant :

$$\mathcal{B} \equiv \frac{u^2}{2} + \psi_G + \mathcal{H} - \frac{R \Omega^*(a) B_\phi}{4\pi \kappa(a)} \quad \text{« Benoulli invariant »}$$



# Back to the accretion problem

Angular momentum conservation:

$$\overline{\rho v_r} \frac{\partial}{\partial R} \Omega R^2 + \frac{1}{R} \frac{\partial}{\partial R} R^2 \left[ \overline{\rho v_\phi v_r} - \frac{B_\phi B_r}{4\pi} \right] + R \left[ \overline{\rho v_\phi v_z} - \frac{B_\phi B_z}{4\pi} \right]_{z=-h}^{+h} = 0$$

accretion

radial stress

vertical stress  
(aka wind stress)

Using MHD invariants:

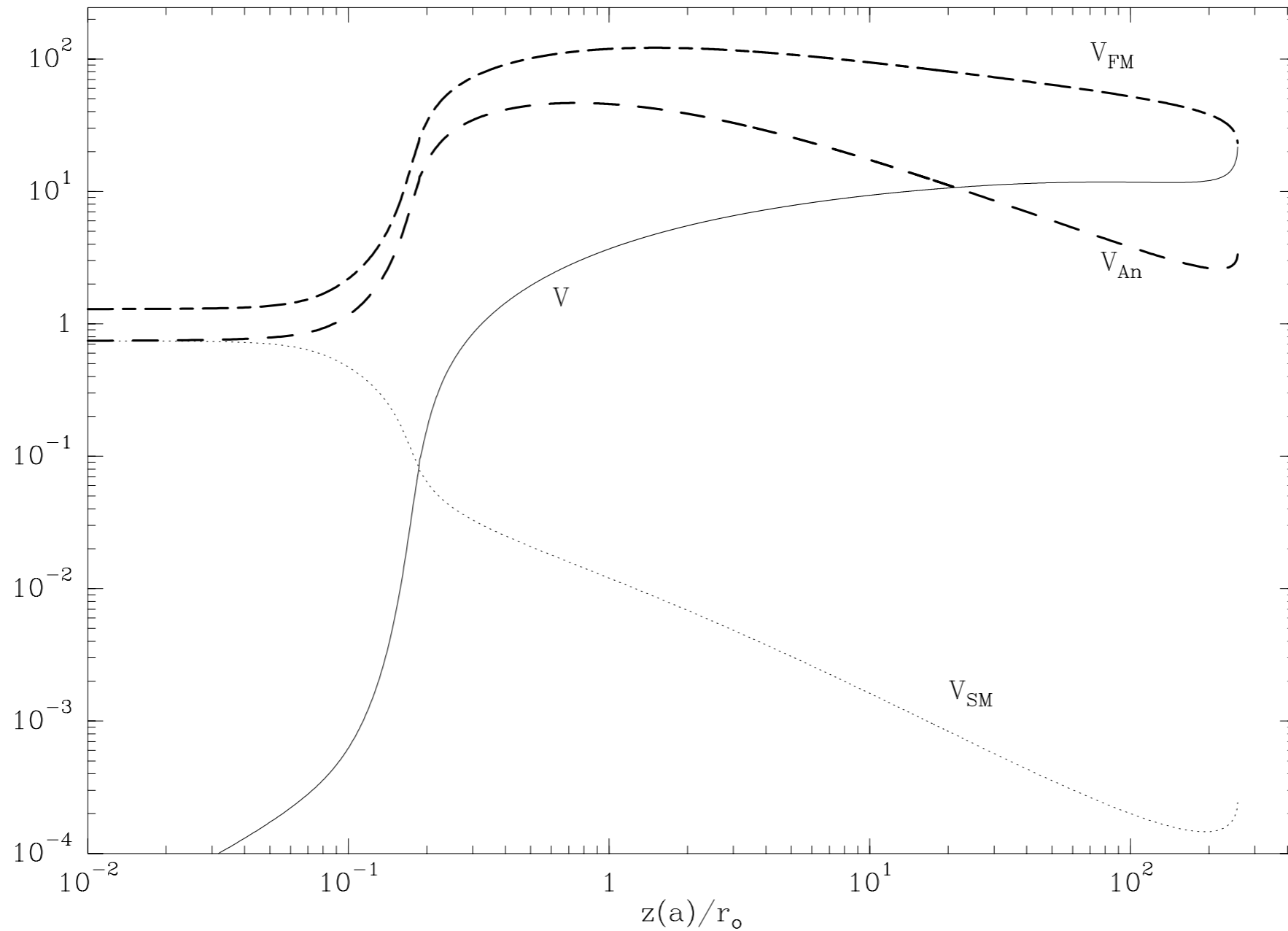
$$R \left[ -\frac{B_\phi B_z}{4\pi} \right]_{-h}^{+h} = R \frac{B_{z0}^2}{4\pi} \kappa (\lambda - 1)$$

Once the MHD invariants are known for a given solution, one can predict the accretion rate, and mass loss rate

# Typical solutions

## Self-similar solutions

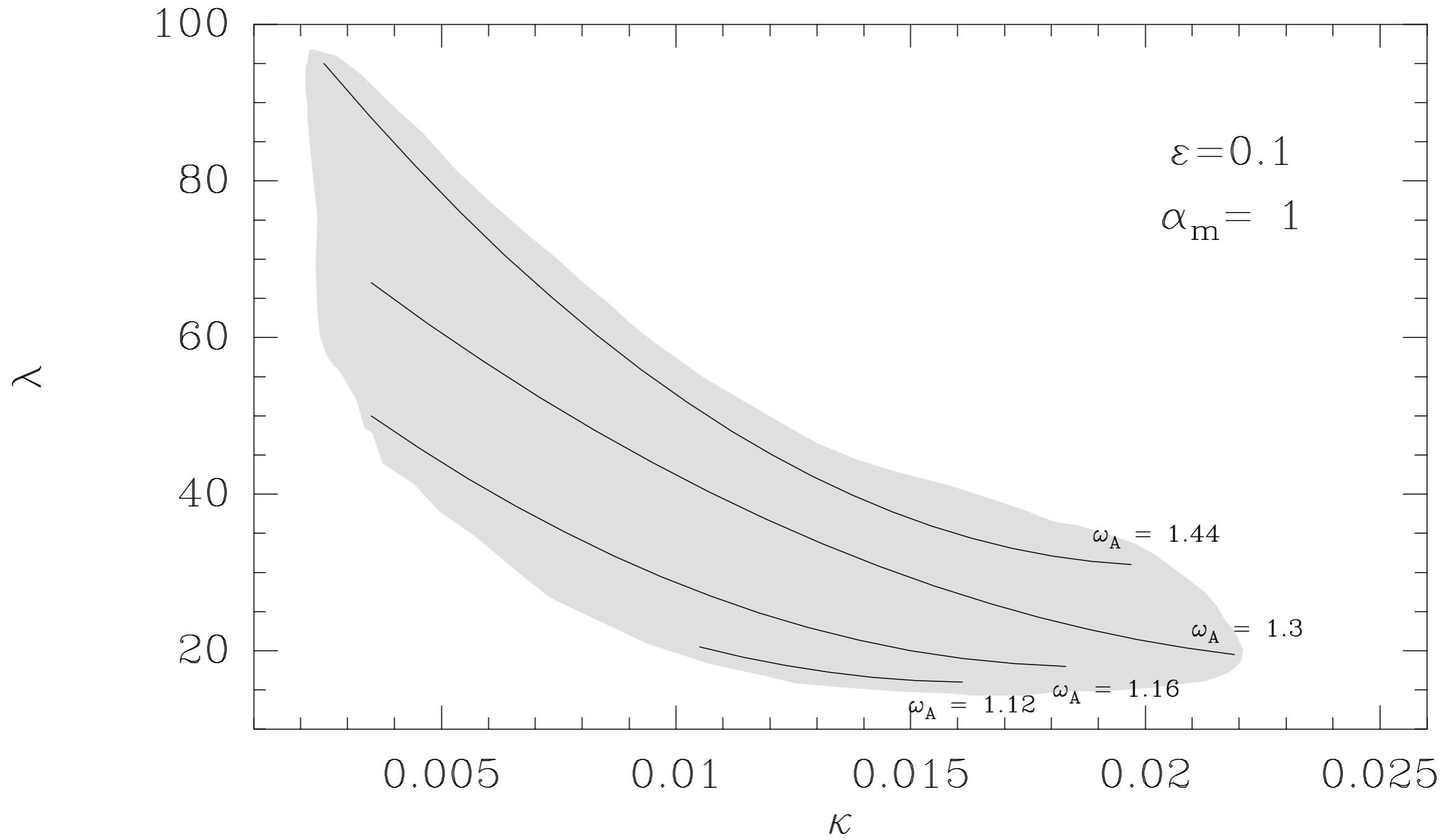
### Typical « cold wind » solution



[Casse & Ferreira 2000]

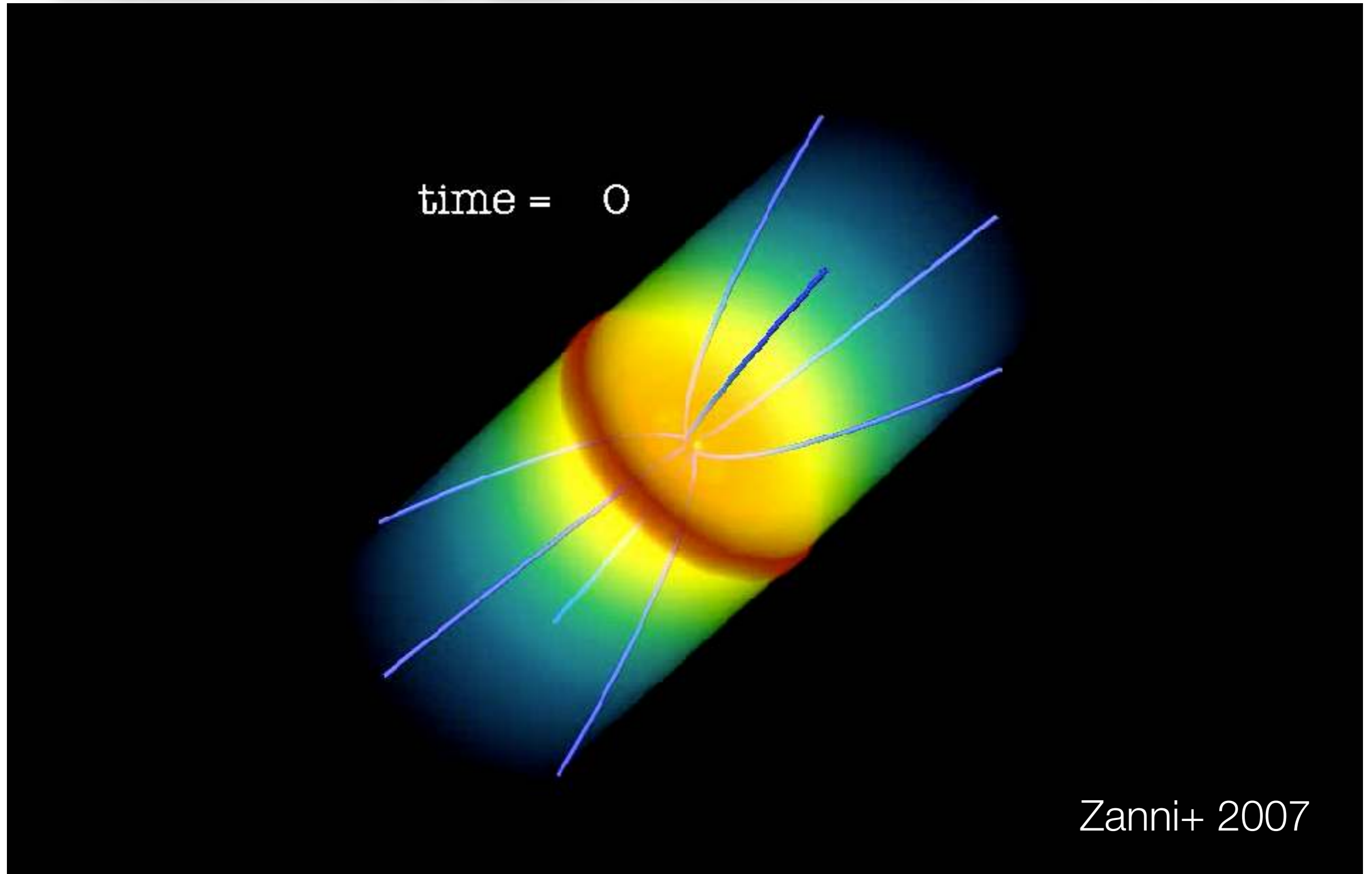
# Typical solutions

## Self-similar solutions



Casse & Ferreira (2000)

# Numerical simulations



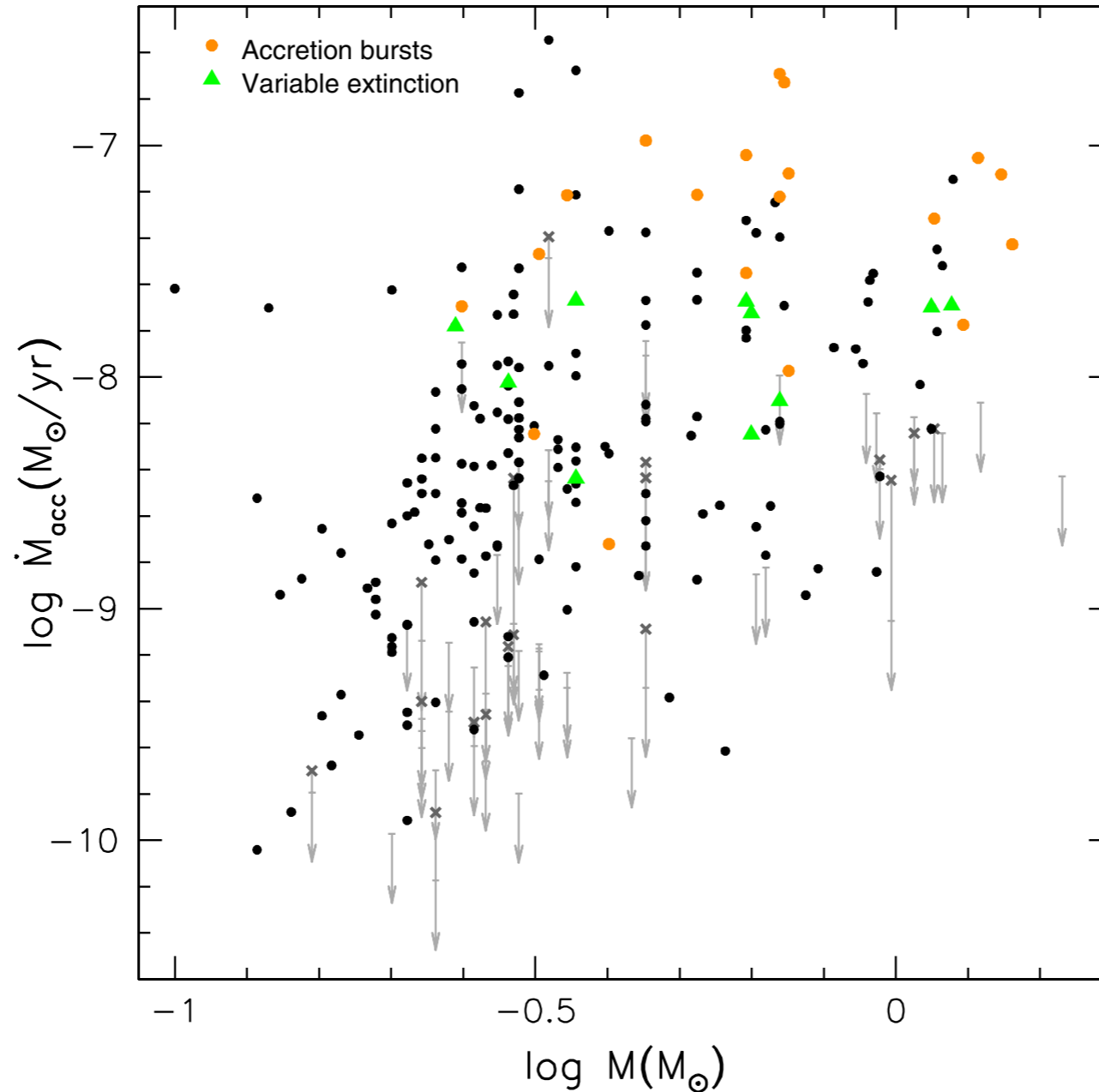
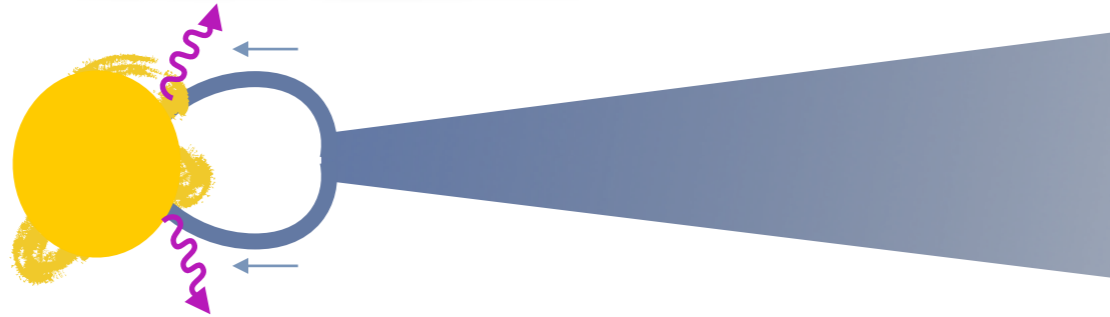
# Overview

---

- A few fun facts about astrophysical discs (10')
- How to drive accretion (30')
- On the difficulty of driving hydrodynamic turbulence (30')
- A short introduction to magnetised wind flows (60')
- Application to protoplanetary discs (20')

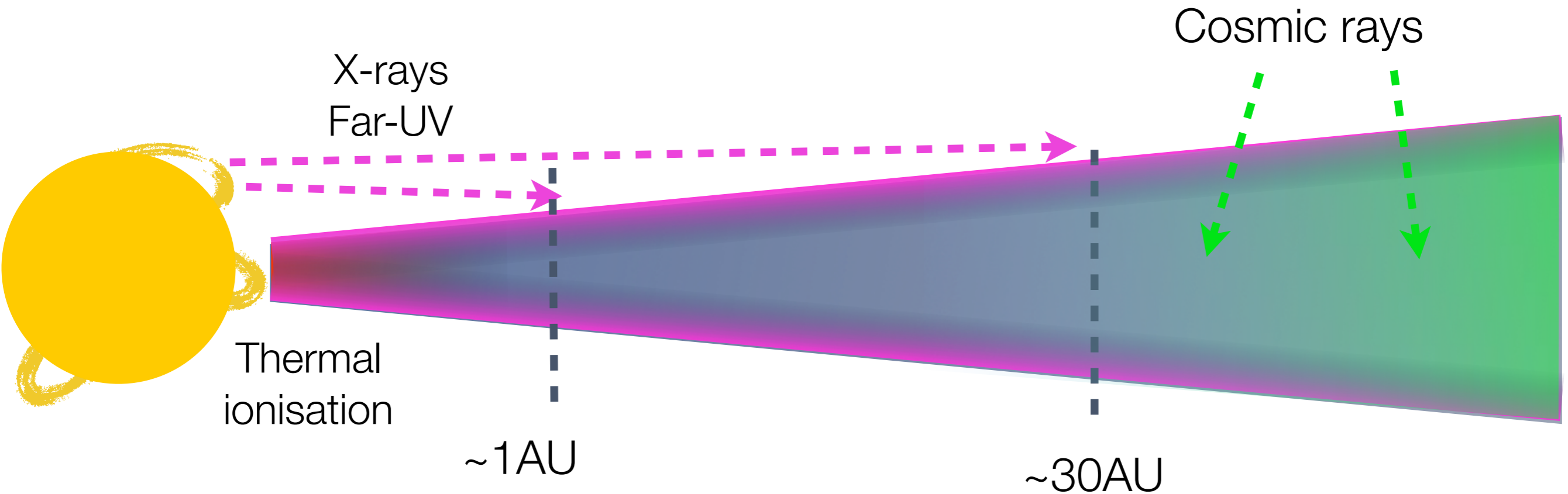


# Accretion rate onto the stellar surface



[Venuti+2014]

# Ionisation sources in protoplanetary discs



« non ideal » MHD effects

- Ohmic diffusion (electron-neutral collisions)
- Ambipolar Diffusion (ion-neutral collisions)
- Hall Effect (electron-ion drift)

Amplitude of these effects depends strongly on location & composition

# Some technical « details » are intentionally hidden...

### 6.3 - MRI in non-ideal MHD

The expression of the non-ideal terms can be interpreted in the following way. First, Ohmic diffusion acts as a pure linear damping operator, as expected. The Hall term is proportional to  $\mathbf{k} \times \mathbf{b}$ , which means it rotates the magnetic perturbation around the  $\mathbf{k}$  direction, keeping its norm constant. Note that the direction of rotation is given by the sign of  $\eta_H$ , which shows that the handedness given by the Hall effect is directly connected to the microphysics of the plasma (see §3.4.1). Finally, ambipolar diffusion involves an anisotropic diffusion term which we will discuss in the following.

The solenoidal conditions can be used to eliminate  $u_x$  and  $b_x$  from the equations in favour of the horizontal components, leading to a 4<sup>th</sup> order problem

$$\begin{aligned} \sigma u_x &= i \frac{\mathbf{k} \cdot \mathbf{B}_0}{4\pi\rho} b_x + 2\Omega \frac{k_z^2}{k^2} u_x, \\ \sigma u_y &= i \frac{\mathbf{k} \cdot \mathbf{B}_0}{4\pi\rho} b_y - (2-q)\Omega u_y, \\ \sigma b_x &= i(\mathbf{k} \cdot \mathbf{B}_0)u_x - \eta_0 k^2 b_x - \eta_H(\mathbf{k} \cdot \widehat{\mathbf{B}}_0)k_z b_y - \frac{\eta_A}{B_0^2} (k^2 B_{0y}^2 b_x - k_x B_{0y}(\mathbf{k} \cdot \mathbf{B}_0)b_y), \\ \sigma b_y &= i(\mathbf{k} \cdot \mathbf{B}_0)u_y - q\Omega b_y - \eta_0 k^2 b_y + \eta_H(\mathbf{k} \cdot \widehat{\mathbf{B}}_0)k_z b_x - \frac{\eta_A}{B_0^2} ((\mathbf{k} \cdot \mathbf{B}_0)^2 + k^2 B_{0y}^2) b_y - \frac{k^2}{k^2} k_x B_{0y}(\mathbf{k} \cdot \mathbf{B}_0)b_x. \end{aligned}$$

### 6.3 - MRI in non-ideal MHD

The expression of the non-ideal terms can be interpreted in the following way. First, Ohmic diffusion acts as a pure linear damping operator, as expected. The Hall term is proportional to  $\mathbf{k} \times \mathbf{b}$ , which means it rotates the magnetic perturbation around the  $\mathbf{k}$  direction, keeping its norm constant. Note that the direction of rotation is given by the sign of  $\eta_H$ , which shows that the handedness given by the Hall effect is directly connected to the microphysics of the plasma (see §3.4.1). Finally, ambipolar diffusion involves an anisotropic diffusion term which we will discuss in the following.

The solenoidal conditions can be used to eliminate  $u_x$  and  $b_x$  from the equations in favour of the horizontal components, leading to a 4<sup>th</sup> order problem

$$\begin{aligned} \sigma u_x &= i \frac{\mathbf{k} \cdot \mathbf{B}_0}{4\pi\rho} b_x + 2\Omega \frac{k_z^2}{k^2} u_x, \\ \sigma u_y &= i \frac{\mathbf{k} \cdot \mathbf{B}_0}{4\pi\rho} b_y - (2-q)\Omega u_y, \\ \sigma b_x &= i(\mathbf{k} \cdot \mathbf{B}_0)u_x - \eta_0 k^2 b_x - \eta_H(\mathbf{k} \cdot \widehat{\mathbf{B}}_0)k_z b_y - \frac{\eta_A}{B_0^2} (k^2 B_{0y}^2 b_x - k_x B_{0y}(\mathbf{k} \cdot \mathbf{B}_0)b_y), \\ \sigma b_y &= i(\mathbf{k} \cdot \mathbf{B}_0)u_y - q\Omega b_y - \eta_0 k^2 b_y + \eta_H(\mathbf{k} \cdot \widehat{\mathbf{B}}_0)k_z b_x - \frac{\eta_A}{B_0^2} ((\mathbf{k} \cdot \mathbf{B}_0)^2 + k^2 B_{0y}^2) b_y - \frac{k^2}{k^2} k_x B_{0y}(\mathbf{k} \cdot \mathbf{B}_0)b_x. \end{aligned}$$

### 3.3 - Single fluid approximation

The equations of motion for charged particles in the frame of the center of mass therefore read

$$q_j \left( \frac{\mathbf{w}_j \times \mathbf{B}}{c} + \mathbf{E}_{cm} \right) - \gamma_{jm} n_j \rho \mathbf{w}_j = 0$$

where we have assumed that dominant collisions were due to neutrals. This is usually recast as

$$\mathbf{w}_j - \mu_j \mathbf{w}_j \times \hat{\mathbf{b}} = \frac{c\mu_j}{B} \mathbf{E}_{cm},$$

where  $\hat{\mathbf{b}}$  is a unit vector parallel to  $\mathbf{B}$  and

$$\mu_j \equiv \frac{q_j B}{\gamma_{jm} m_j c},$$

is the Hall parameter (Wardle & Ng 1999). Equation (4) can be solved for  $\mathbf{w}_j$ , which gives the asymptotic velocity

$$\begin{aligned} \mathbf{w}_{j\parallel} &= \frac{c\mu_j}{B} \mathbf{E}_{cm\parallel}, \\ \mathbf{w}_{j\perp} &= \frac{c\mu_j}{B(1+\mu_j^2)} \left[ \mathbf{E}_{cm\perp} + \mu_j \mathbf{E}_{cm\perp} \times \hat{\mathbf{b}} \right]. \end{aligned}$$

We eventually obtain an expression closing our set of equations by relating the drift velocities to the current in the flow  $\mathbf{J} = \sum_j n_j q_j \mathbf{w}_j$  and assuming quasi-neutrality  $\sum_j n_j q_j = 0$ :

$$\begin{aligned} \mathbf{J}_{\parallel} &= \frac{c}{B} \left( \sum_j q_j n_j \mu_j \right) \mathbf{E}_{\parallel}, \\ \mathbf{J}_{\perp} &= \frac{c}{B} \left( \sum_j \frac{q_j n_j \mu_j}{1+\mu_j^2} \right) \mathbf{E}_{cm\perp} + \frac{c}{B} \left( \sum_j \frac{q_j n_j}{1+\mu_j^2} \right) \hat{\mathbf{b}} \times \mathbf{E}_{cm\perp}. \end{aligned}$$

These expressions constitute the base of Ohm's law. We can identify 3 conductivity tensors: the Ohmic, Hall and Petersen conductivity tensors:

$$\begin{aligned} \sigma_o &= \frac{c}{B} \sum_j q_j n_j \mu_j, \\ \sigma_H &= \frac{c}{B} \sum_j \frac{q_j n_j}{1+\mu_j^2}, \\ \sigma_P &= \frac{c}{B} \sum_j \frac{q_j n_j \mu_j}{1+\mu_j^2}, \end{aligned}$$

defined so that Ohm's law can be written in the more familiar form:

$$\mathbf{J} = \sigma_{\parallel} \mathbf{E}_{cm\parallel} + \sigma_H \hat{\mathbf{b}} \times \mathbf{E}_{cm\perp} + \sigma_P \mathbf{E}_{cm\perp}$$

This relation can be inverted one final time to obtain the electric field in the observer frame and write the induction equation as

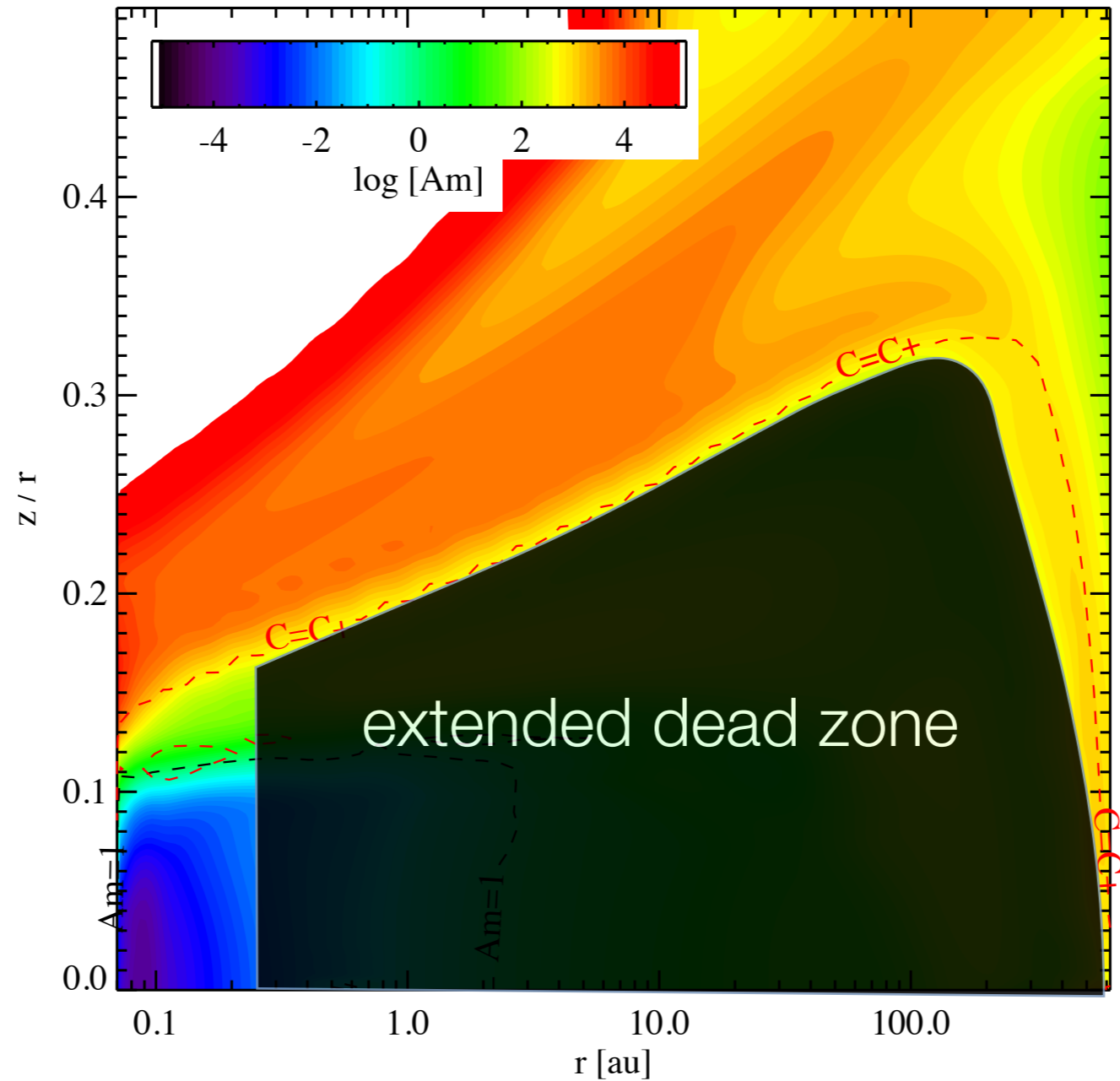
$$\frac{\partial \mathbf{B}}{\partial t} = \nabla \times (\mathbf{v} \times \mathbf{B}) - \nabla \times (\eta_o \nabla \times \mathbf{B} + \eta_H (\nabla \times \mathbf{B}) \times \hat{\mathbf{b}} + \eta_A (\nabla \times \mathbf{B})_{\perp})$$

Figure 20: Physical principle of the Hall-shear instability (HSI). The magnetic perturbation (in green) is rotated clockwise or counter-clockwise by the Hall effect depending on the polarity of the mean field  $B_0$  (top/bottom). When  $B_0 > 0$ , the rotated perturbation of a whistler wave shear (in blue) while it is damped by the shear when  $B_0 < 0$ .

This instability is a result of sheared whistler waves. If we look at the disc from the side pointing towards us, the magnetic perturbation of a whistler wave shear (in blue) while it is damped by the shear when  $B_0 < 0$ .

34

# Ambipolar diffusion



→  $Am < 100$  → « damped » MRI

What do observers say?

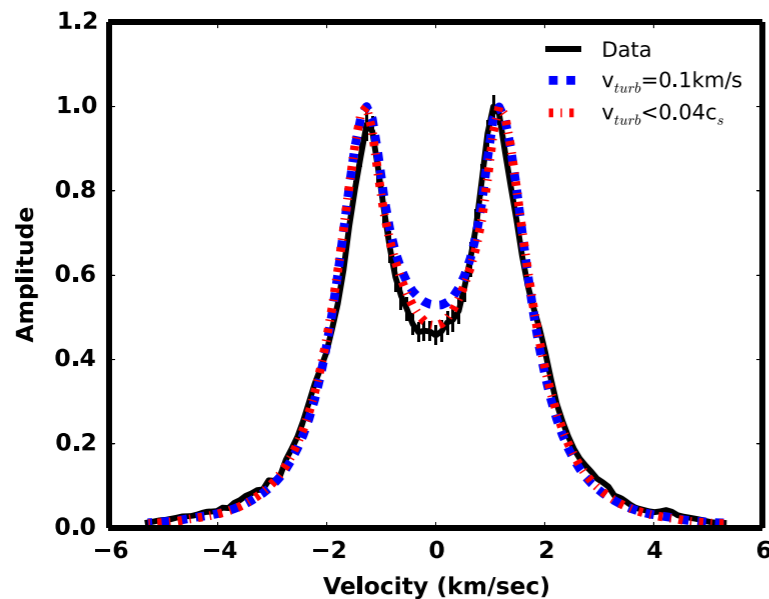


# Line broadening

● Emission lines from the gas are broadened by:

- Keplerian rotation  $V_k$
- Thermal velocity  $v_{th} \simeq c_s \ll V_k$
- Turbulence  $v_{turb} \simeq \sqrt{\alpha} c_s$

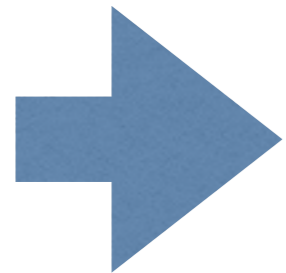
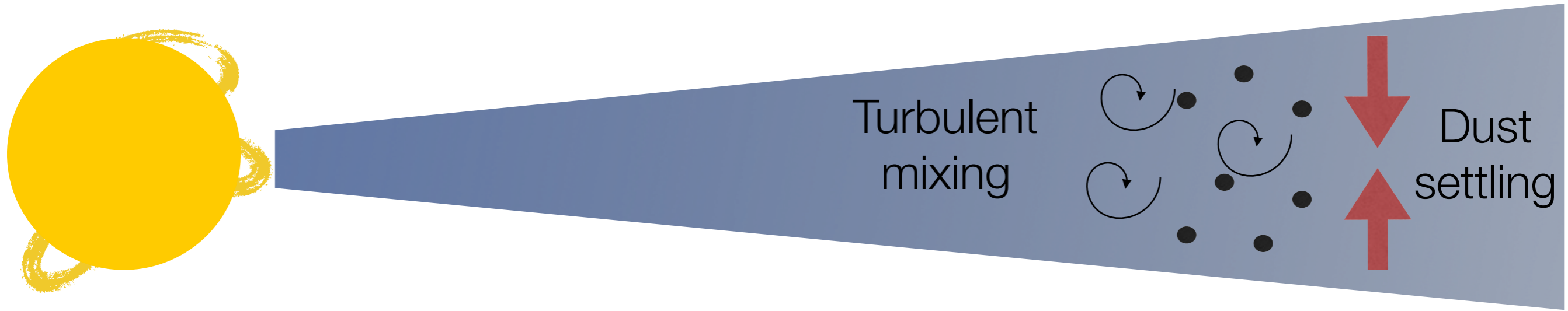
Measuring line broadening due to turbulence requires very precise measures/estimates of  $V_k$  and  $c_s$



Turbulence velocity smaller than  $0.04 c_s$

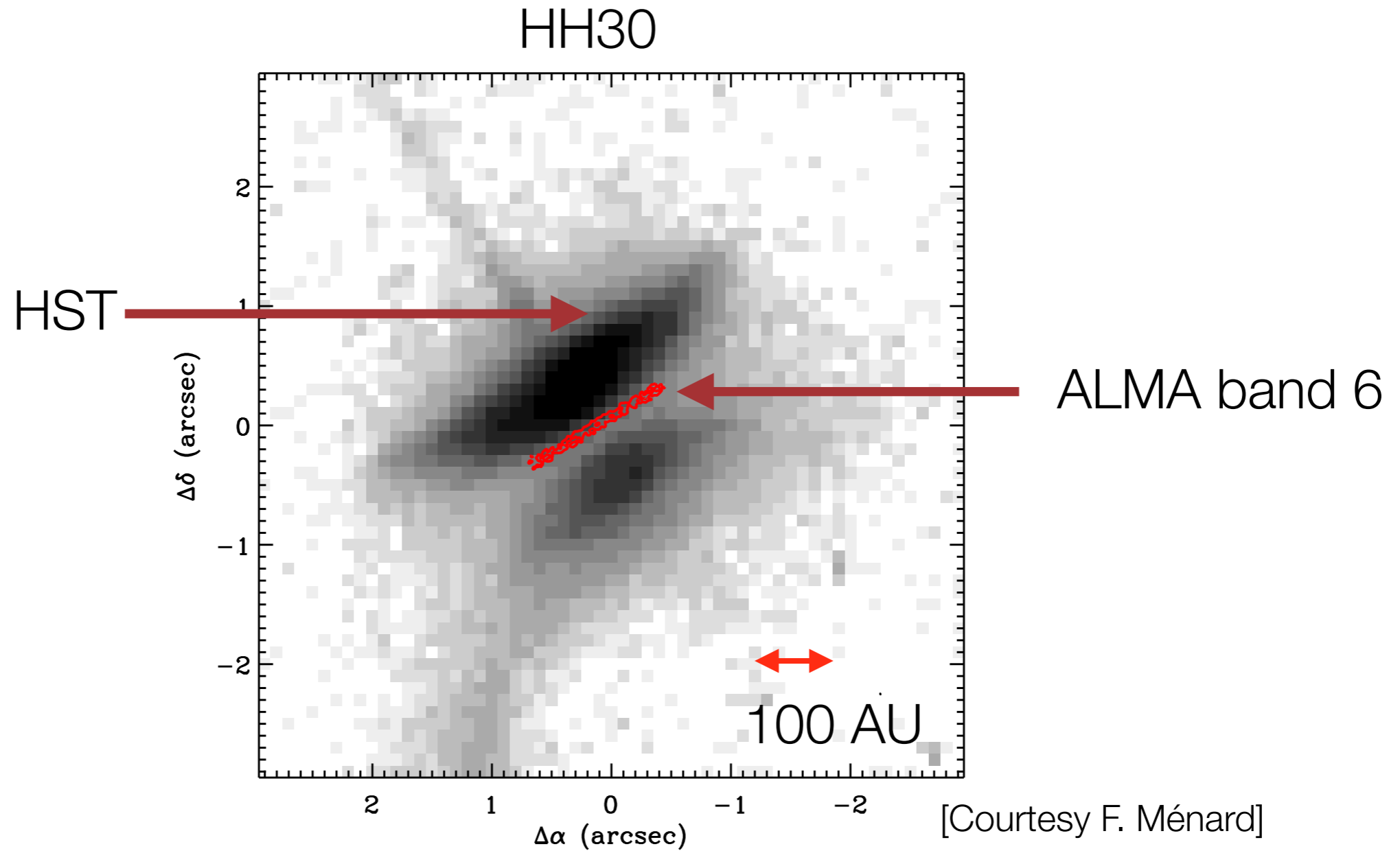
**Figure 6.** CO(3-2) high resolution spectra (black line) compared to the median model when turbulence is allowed to move toward very low values (red dotted-dashed lines) or when it is fixed at  $0.1 \text{ km s}^{-1}$  (blue dashed lines). All spectra have been normalized to their peak flux to better highlight the change in shape. The models with weak turbulence provide a significantly better fit to the data despite the fact that the turbulence is smaller than the spectral resolution of the data.

# Dust settling (I)



The thickness of the dust layer depends on the competition between settling and turbulent mixing

# Dust settling in edge on discs



mm-sized dust grains are strongly settled  low level of turbulence

# Summary: Failure of the turbulent disc model

## Theoretical

Discs are very weakly ionised

- “Non-ideal” MHD effects
- MHD turbulence too weak to explain observed accretion rates [Turner+2014, PPVI]

## Observational

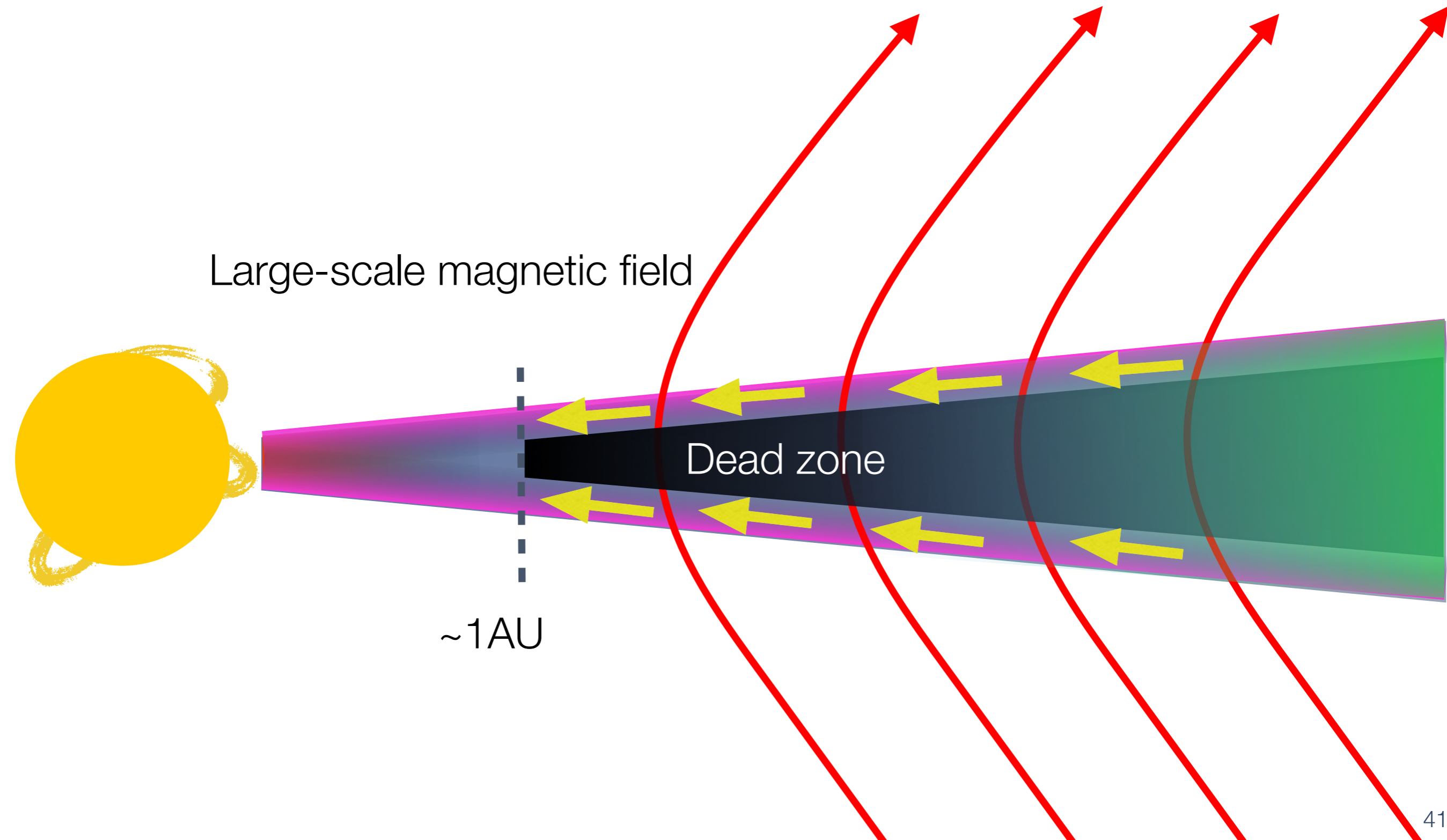
- Turbulent line broadening (CO, DCO+) smaller than expected from MHD turbulence [Flaherty+2015, 2017]
- Vertical dust settling stronger than expected from MHD turbulence [Pinte+2016]
- Turbulence (if it exists) is much weaker than anticipated in the turbulent disc model

## Key questions

- What drives accretion in protoplanetary discs?
- Which process is responsible for the large scale structures we observe?

# Wind-driven accretion in magnetically « dead » discs

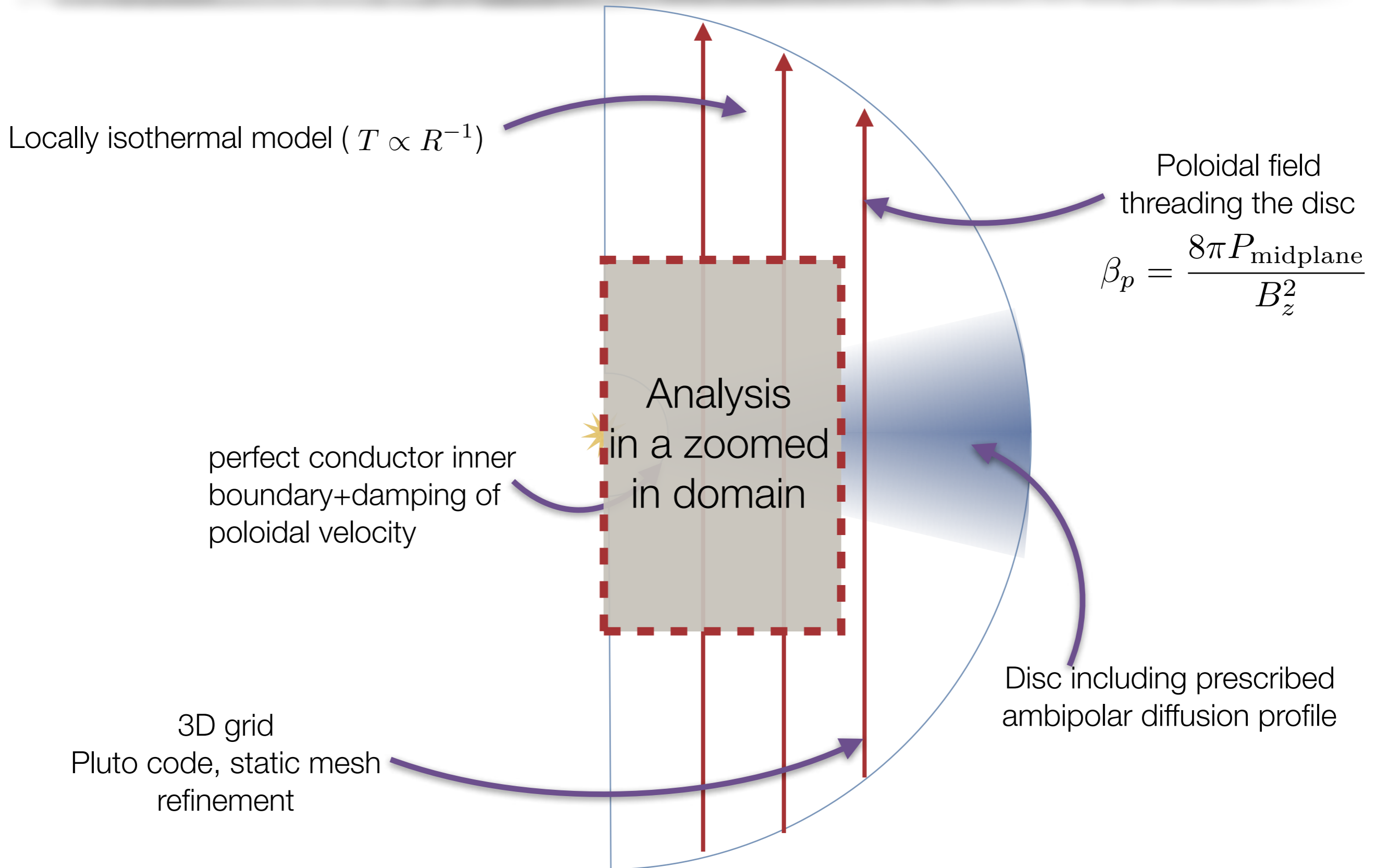
[Wardle & Konigl 1993, Bai+ 2013, Lesur+ 2014, Simon+ 2015 in local models, Gressel+2015, Béthune+2017, Bai 2017, Wang+ 2018, ... in global geometry]





# Global simulations

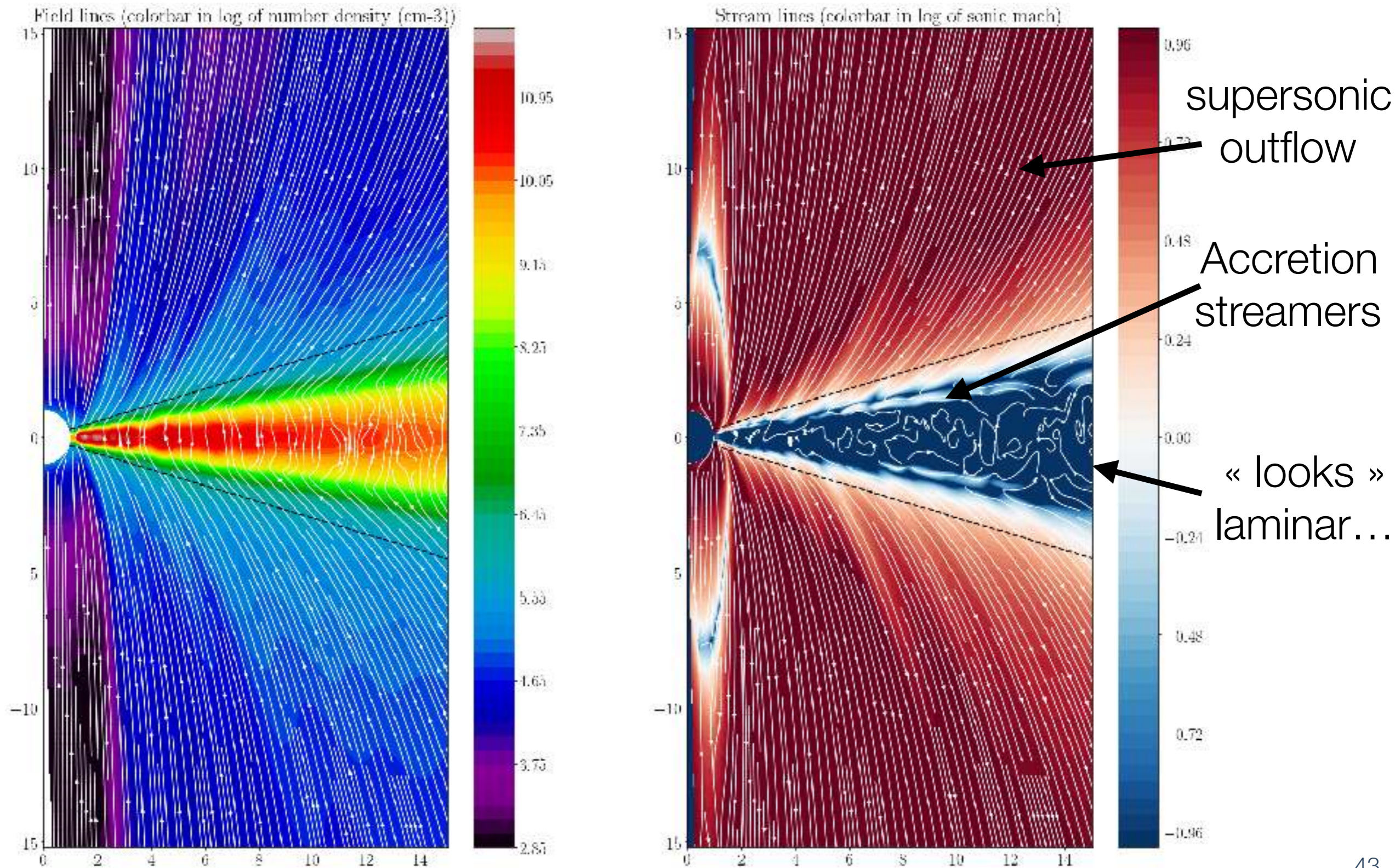
## Numerical setup





# Global picture

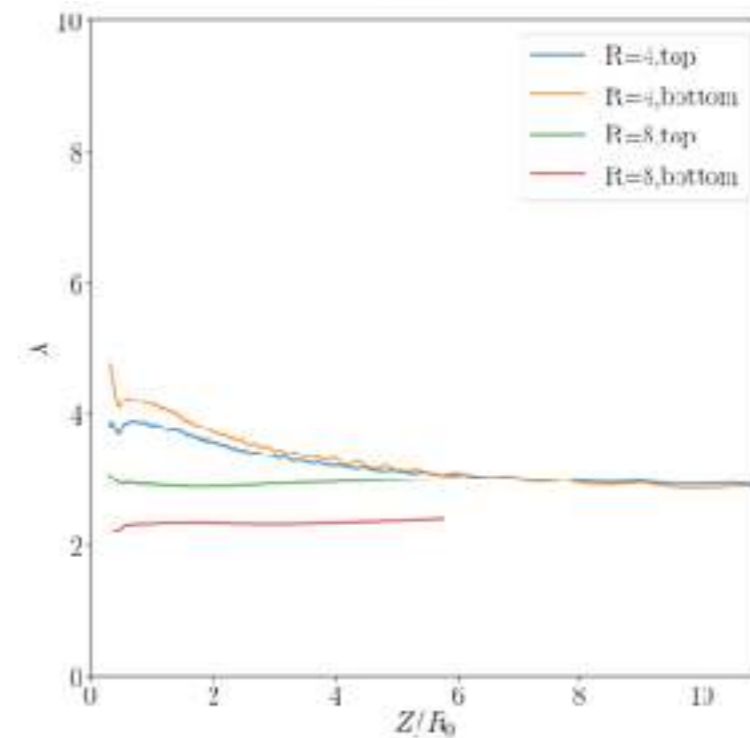
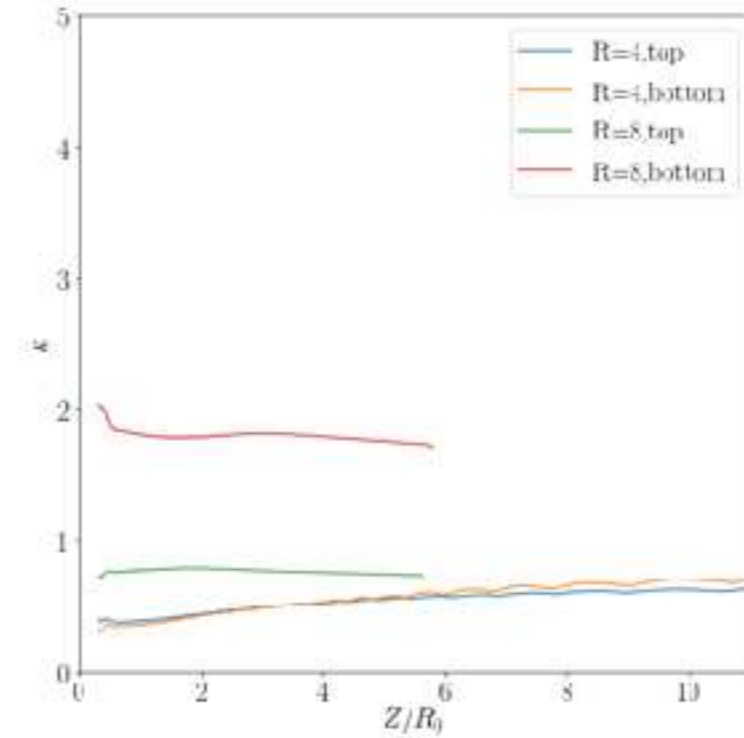
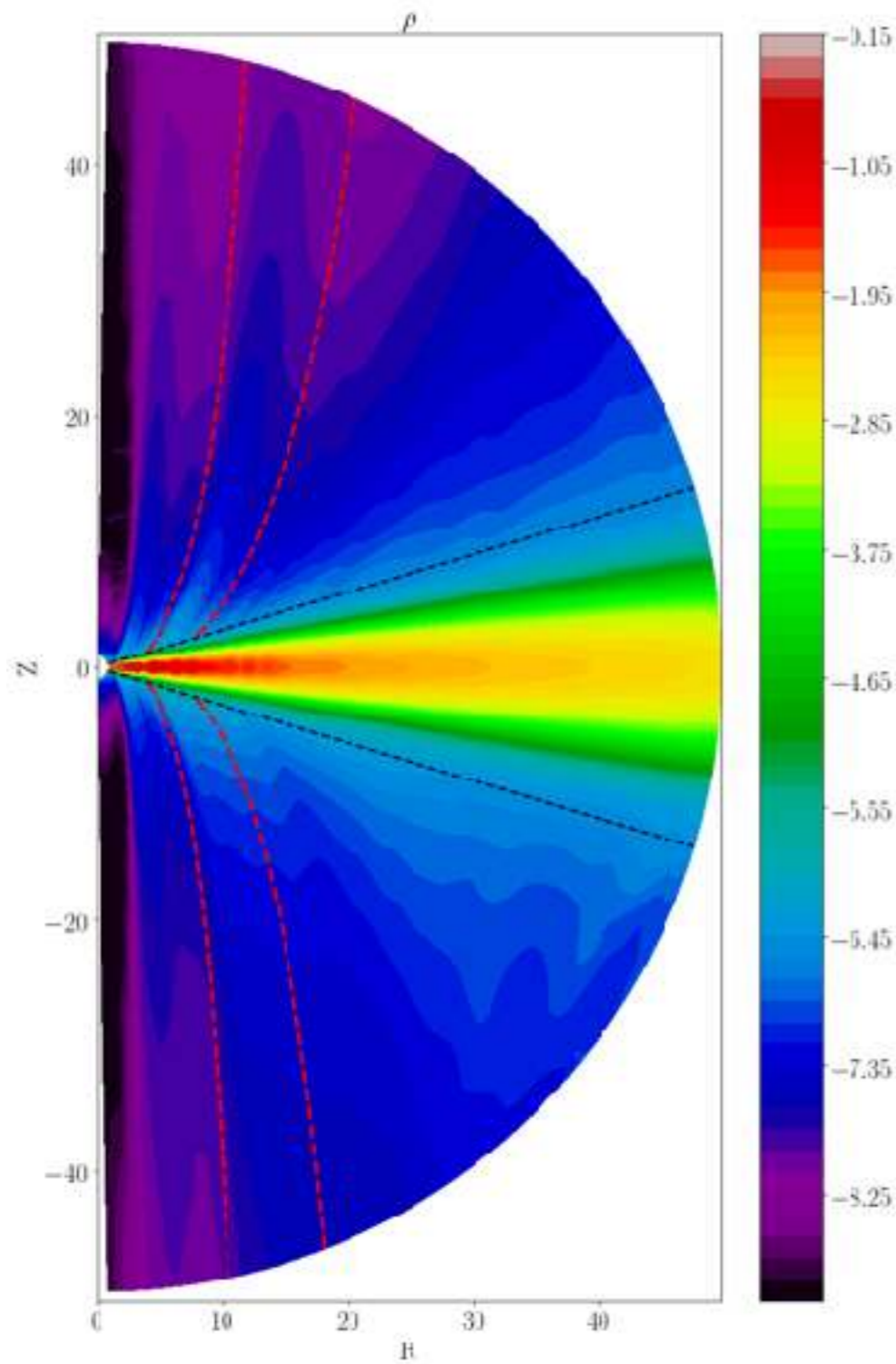
$\beta_p = 10^4$ ,  $Am_{\text{mid}} = 1$  average from  $t=1700$  orbits to  $t=2400$  orbits





# Wind invariants

Take 4 representative streamlines and compute ideal MHD invariants



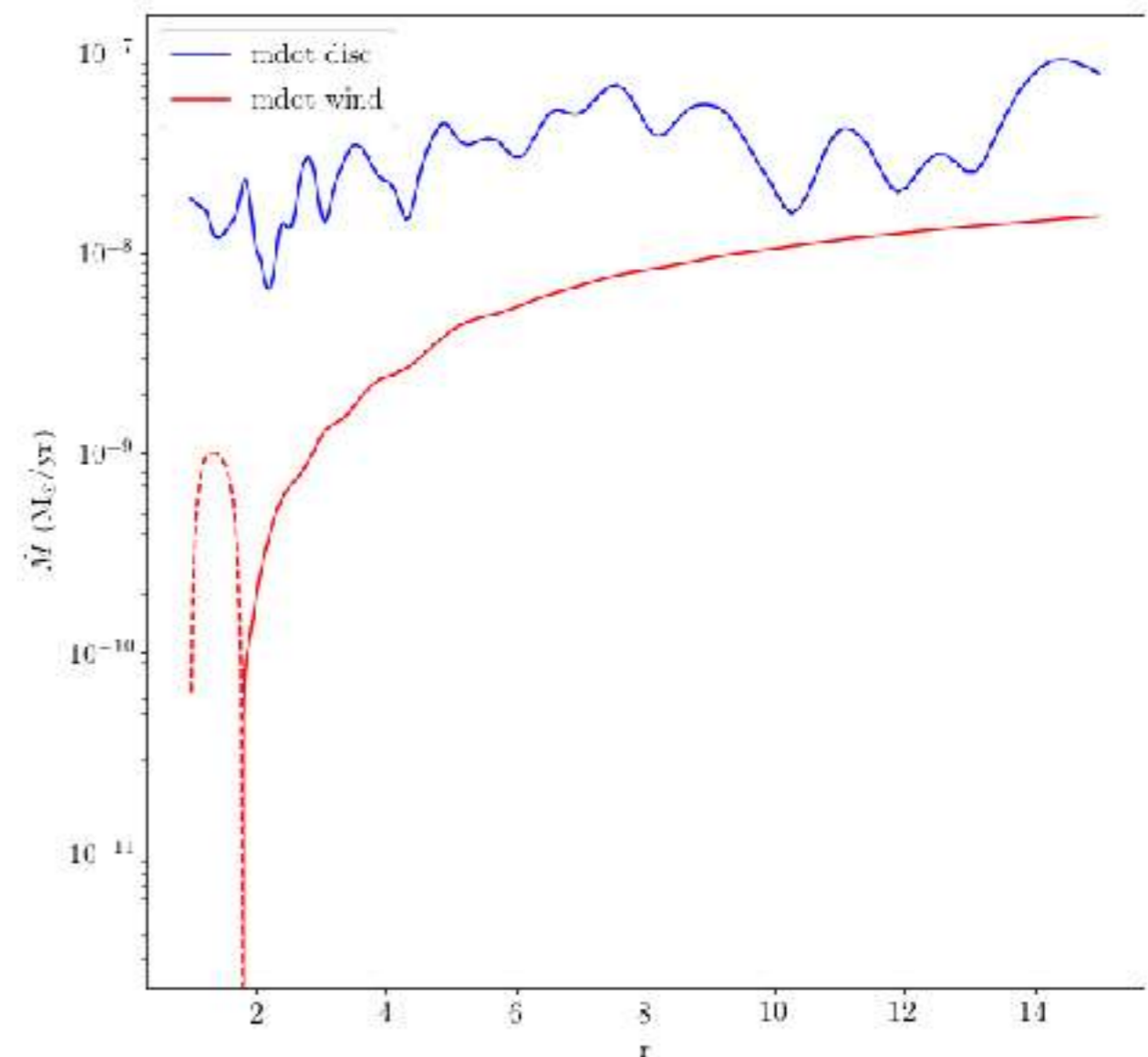
# Accretion rate, mass loss rate

- Typical accretion rate  $\sim 10^{-8}—10^{-6} M_{\odot}/\text{yr}$
- Accretion rate mostly controlled by the magnetic flux  $\dot{M} \propto \beta^{-(0.5—1)}$
- Wind efficiency defined from

$$\dot{M}_{\text{wind}} = \int_{R_{\text{in}}}^R dR R [\rho u_z]_{\text{surface}}$$

$$\xi = \frac{1}{\dot{M}} \frac{d\dot{M}_{\text{wind}}}{d \log R}$$

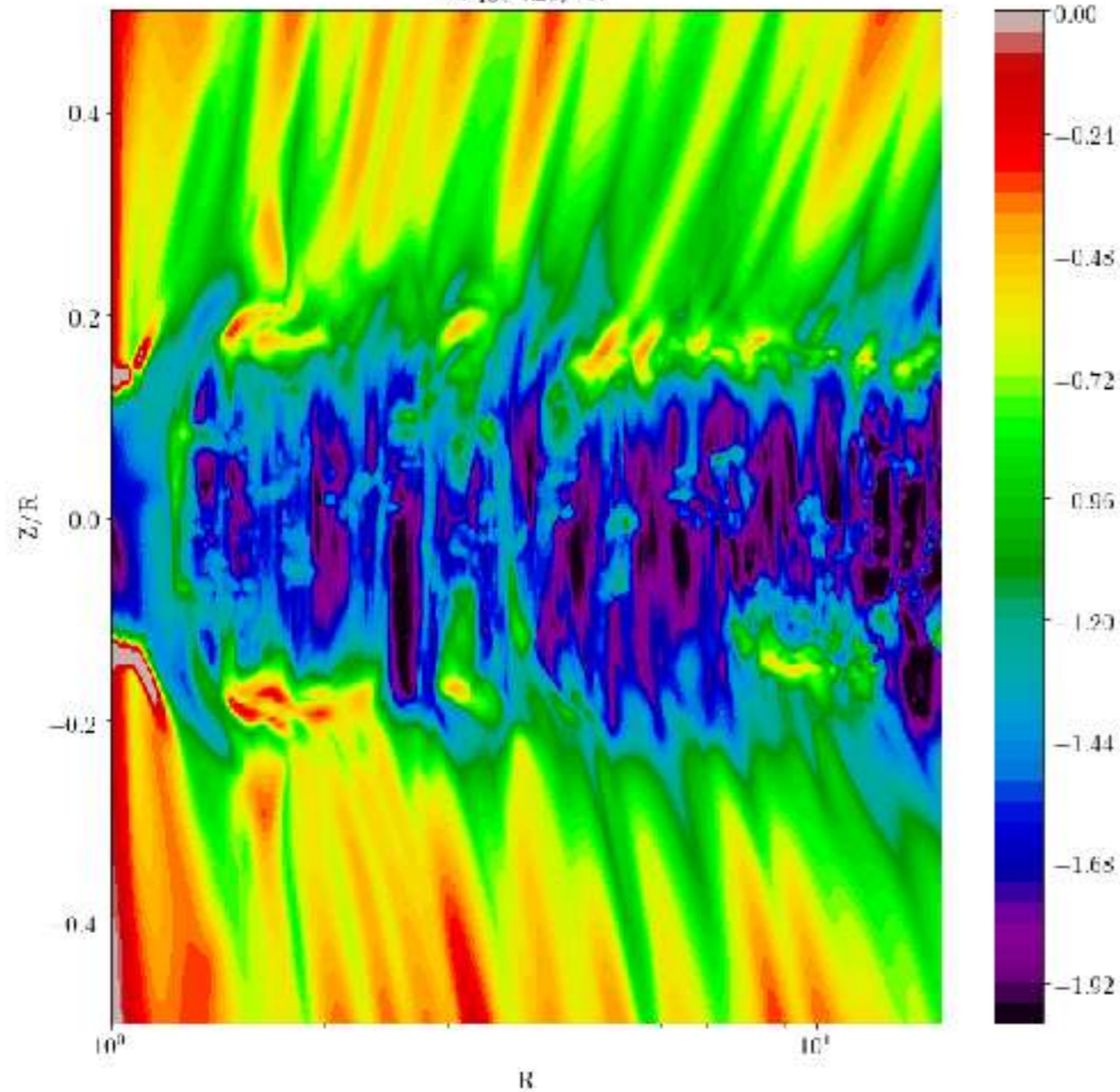
- Typically have  $\xi = 0.2—1$   
corona heating leads to larger  $\xi$   
[Casse & Ferreira 2000, Béthune+2017, Bai 2017, Wang+2018]



# Turbulence?

$$v_{\text{turb}} = \left\langle \left( v - \langle v \rangle \right)^2 \right\rangle^{1/2}$$

$C_{\text{turb}}(v_{\text{turb}}/c_s)$

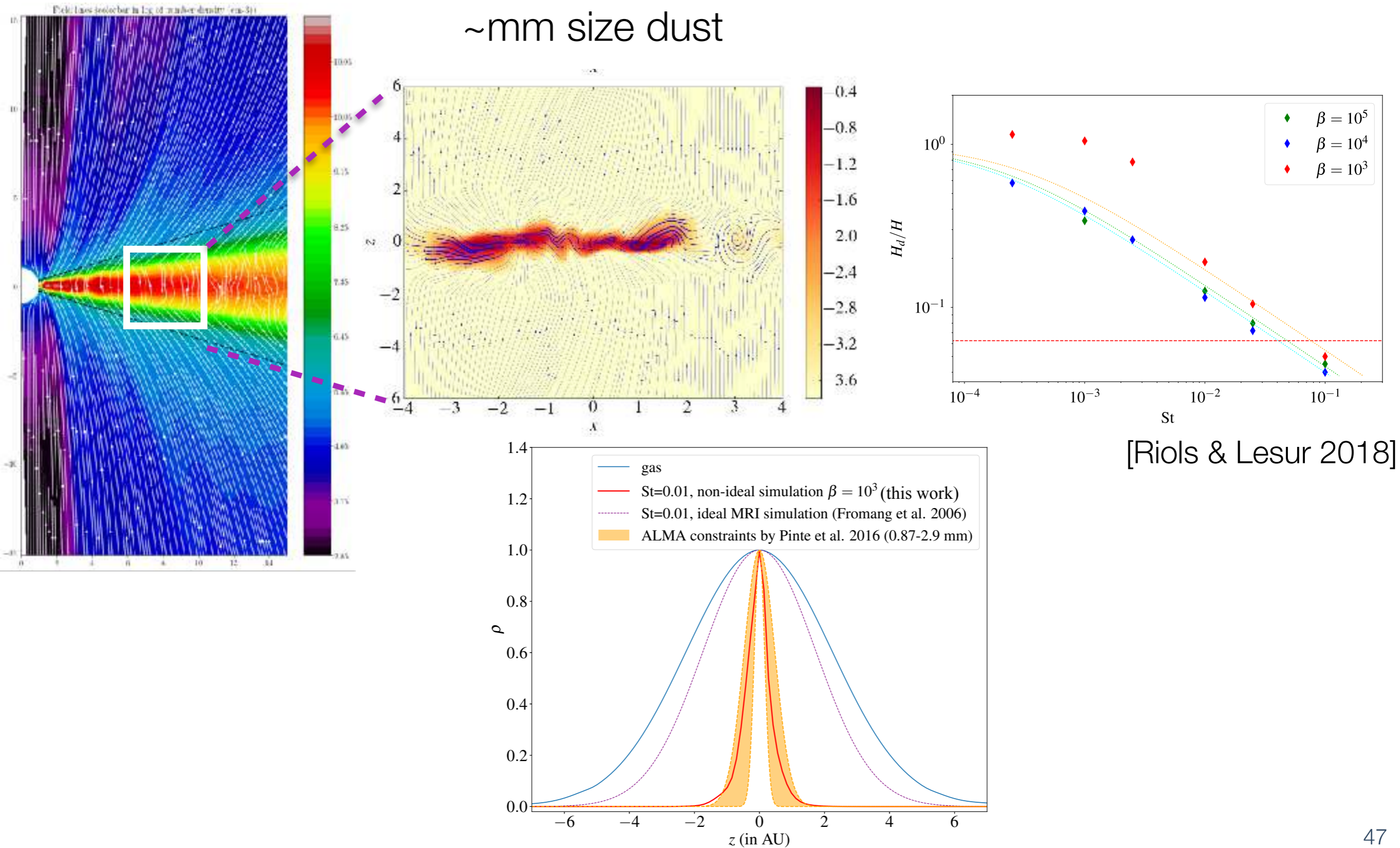


Typical velocity fluctuations of the order of 1% of the sound speed

Compatible with observed turbulent broadening of CO lines



# Dust Dynamics @ 30 AU

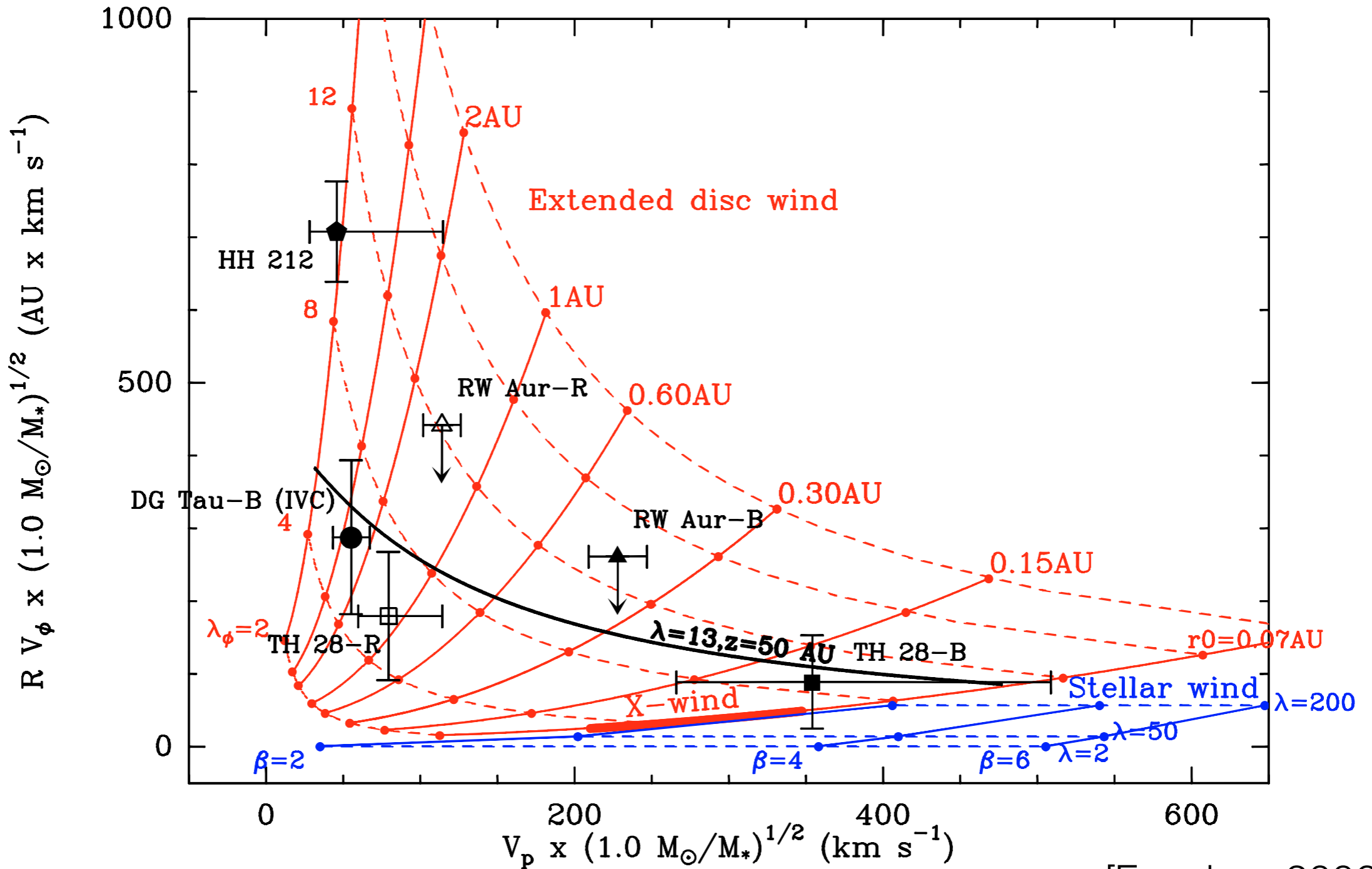


# A few take away points

---

- Astrophysical discs can be accreting thanks to anomalous viscosity (turbulence, waves), or magnetised winds
- shear-driven hydrodynamic turbulence is notoriously difficult to trigger in Keplerian flows
- Winds are full non linear solution to the MHD equations. They require a large scale poloidal field, and some magnetic diffusion in the disc (to allow for accretion)
- In protoplanetary discs:
  - magnetic diffusion suppresses the MRI, but it provides the diffusion required by wind solutions.
  - these laminar wind solutions naturally reproduce some of the observed features of these discs: accretion rate, low level of turbulence, strong dust settling.

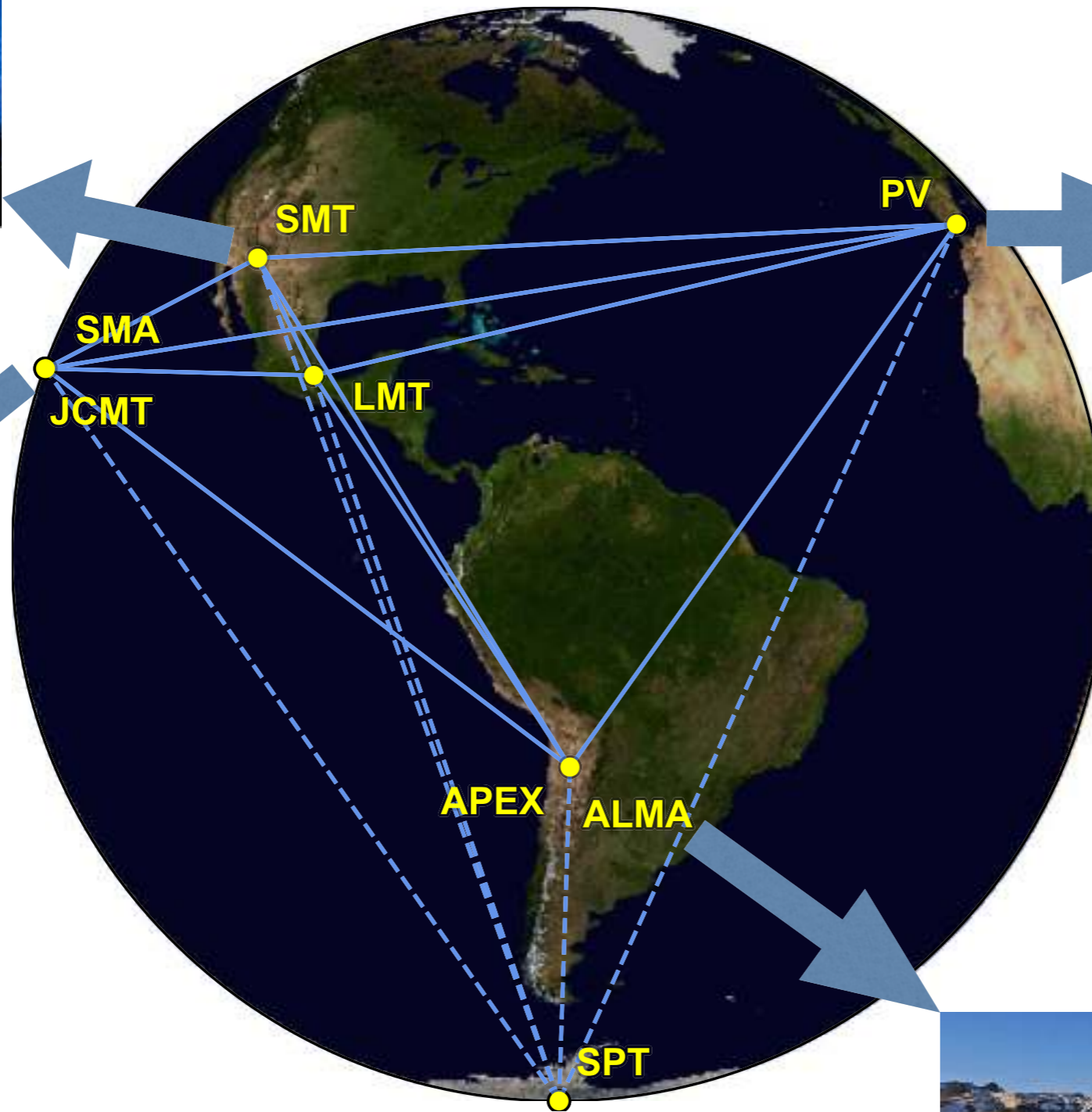
# Testing jets kinematics



[Ferreira+ 2006]



# Observing M87



# Ejection evidence in HL tau

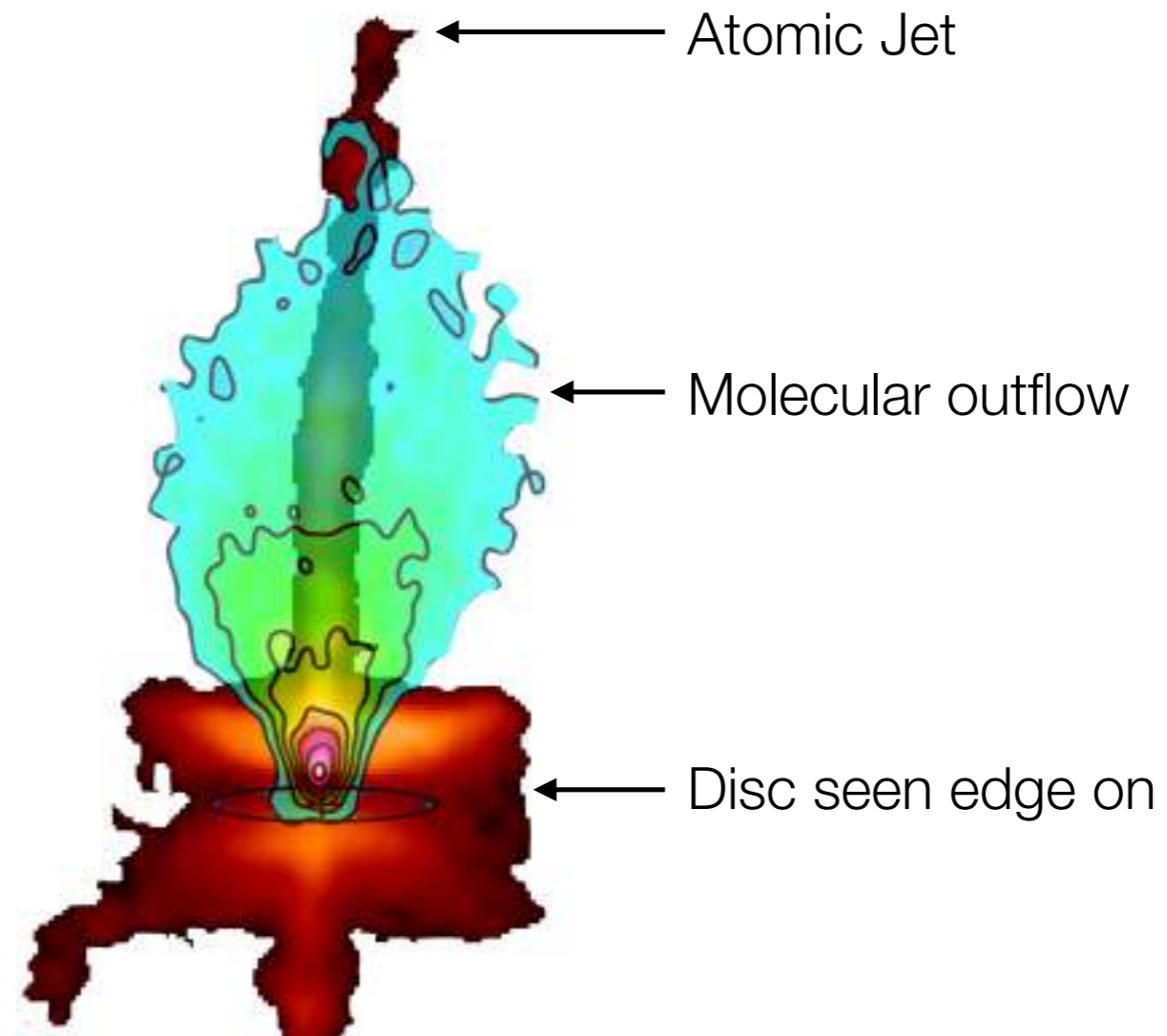


Figure 3: Observation of an atomic jet and a molecular wind observed in CO(2-1) by ALMA in HH30, a protoplanetary disc seen edge-on. Courtesy of C. Dougados (Dougados et al. 2017).